



1 **Tectonothermal evolution in the core of an arcuate fold and**
2 **thrust belt: the southeastern sector of the Cantabrian Zone**
3 **(Variscan belt, NW Spain)**

4 M. L. Valín, S. García-López, C. Brime, F. Bastida and J. Aller

5 Departamento de Geología, Universidad de Oviedo, 33005 Oviedo, Spain

6 *Correspondence to:* Fernando Bastida (bastida@geol.uniovi.es)

7 **Abstract.** The tectonothermal evolution of an area located in the core of the Ibero-Armorican arc (Variscan belt)
8 has been determined by using the conodont color alteration index (CAI), Kübler index of illite (KI), the Árkai
9 index of chlorite (AI), and the analysis of clay minerals and rock cleavage. The area is part of the Cantabrian
10 Zone (CZ), which represents the foreland fold and thrust belt of the orogen. It has been thrust by several large
11 units of the CZ, what resulted in the generation of a large amount of synorogenic Carboniferous sediments. CAI,
12 KI and AI values show an irregular distribution of metamorphic grade, independent of stratigraphic position.
13 Two tectonothermal events have been distinguished in the area. The first one, poorly defined, is mainly located
14 in the northern part. It gave rise to very low-grade metamorphism in some areas and it was associated with a
15 deformation event that resulted in the emplacement of the last large thrust unit and development of upright folds
16 and associated cleavage (S_1). The second tectonothermal event gave rise to low-grade metamorphism and
17 cleavage (S_2) crosscutting earlier upright folds in the central, western and southern parts of the study area. The
18 event continued with the intrusion of small igneous rock bodies, which gave rise to contact metamorphism and
19 hydrothermal alteration. The second event was linked to an extensional episode due to a gravitational instability
20 at the end of the Variscan deformation. This tectonothermal evolution occurred during the Gzhelian-Sakmarian.
21 Subsequently, several hydrothermal episodes took place, in association with local development of crenulation
22 cleavage during the Alpine deformation.

23 **1 Introduction**

24 The Variscan belt defines an arc in the northwestern Iberian Peninsula (Ibero-Armorican Arc), whose core is
25 formed by the Cantabrian Zone (CZ), which represents the foreland fold and thrust belt of the orogen (Fig. 1).
26 This zone consists of Palaeozoic rocks in which two tectonostratigraphic units have been distinguished (Julivert,
27 1978; Marcos and Pulgar, 1982), whose limit is approximately located by the Devonian-Carboniferous
28 boundary. The preorogenic unit is formed of Cambrian to Devonian rocks consisting of alternating carbonate and
29 siliciclastic formations; they form a wedge that thins towards the foreland. The synorogenic unit is formed by
30 several clastic units, also thinning towards the foreland, which filled foredeep basins generated in the front of the
31 main thrust units of the CZ. In this zone, the Variscan deformation occurred during the upper Carboniferous and
32 gave rise to thin-skinned tectonics, with several large thrust units and associated folds (Fig. 1); the units were
33 emplaced in a sequence towards the foreland. The deformation occurred under shallow crustal conditions, so that
34 diagenetic conditions are dominant in the zone and absence of cleavage in the rocks is also dominant.
35 Nevertheless, there are several areas of the CZ where cleavage and very low- or low-grade metamorphism are



36 present. One of these areas is the southeastern sector of the Cantabrian Zone. It is a foreland basin that occupies
37 the core of the Ibero-Armorican Arc, and has undergone, a complex history of sedimentation, deformation,
38 metamorphism, and to a lesser extent, magmatism.

39 The present study aims to present a model of tectonothermal evolution for the core of the Ibero-Armorican
40 arc based on conodont colour alteration index (CAI), the Kübler index (KI) of illite, the Árkai index (AI) of
41 chlorite, the analysis of clay minerals and the rock cleavage development.

42 2 Geological setting

43 The southeastern sector of the Cantabrian Zone is made up of two units: the Pisuega-Carrión unit (PCU) and the
44 Valsurbio unit (VU) (Fig. 1). As a consequence of its location in the core of the Ibero-Armorican arc, the PCU
45 has been thrust over successively by the VU, the Central Coal Basin, the Ponga unit and the Picos de Europa
46 unit, (Fig. 1). Thus, the PCU operated as a foreland basin during a great part of the history of the Variscan
47 deformation. This history involved the accumulation of a great thickness of synorogenic Carboniferous
48 sediments, corresponding to clastic wedges associated with the exhumation of the thrust units.

49 The VU is located to the south of the PCU. Marine facies occur in both units, but from the Emsian, the
50 sediments in the latter unit were deposited in deeper waters than those in the former unit. The VU represents an
51 extension of the southern part of the CZ, and presents a Devonian succession comparable to that of that part
52 (Koopmans, 1962). The units containing Silurian-Devonian rocks located within the PCU have been interpreted
53 as transported from internal areas of the orogenic belt, specifically from the southeastern extension of the
54 Westasturian-Leonese Zone, currently hidden under the Mesozoic-Cenozoic cover of the Duero basin, and
55 located to the south of the VU (Frankenfeld, 1983; Marquínez and Marcos, 1984; Rodríguez Fernández and
56 Heredia, 1987; Rodríguez Fernández, 1994). These units were named 'Palentine nappes' by Rodríguez
57 Fernández and Heredia (1987). The PCU and the VU are separated by the León fault (also called 'Ruesga fault'
58 in the study area) (Fig. 2), that traverses most of the Cantabrian Zone and whose meaning is controversial (de
59 Sitter, 1962; Marcos, 1968, 1979; Julivert et al., 1971; Kullmann and Schöenberg, 1978, 1979; Heward and
60 Reading, 1980; Aller, 1986; Rodríguez Fernández and Heredia, 1988; Nijman and Savage, 1989; Rodríguez
61 Fernández, 1991; Alonso et al., 2009, 2012).

62 The oldest sediments of the study area are Silurian (Wenlock-Pridoli) sandstones and lutites. The Devonian
63 rocks consist of an alternation of carbonate and siliciclastic formations with the facies differences cited above.
64 Mississippian rocks are mainly limestones in the lower part, especially in the VU; upwards a mostly turbiditic
65 sequences appears with common olistoliths in the northern sector and some carbonate levels. The Pennsylvanian
66 succession is dominantly siliciclastic, with a thickness of several thousand meters and synorogenic character. In
67 relation to this synorogenic sedimentation, several syntectonic unconformities have been described, among
68 which the Curavacas unconformity (early Moscovian) can be highlighted by its structural significance (Van
69 Veen, 1965; Lobato 1977; Alonso and Rodríguez Fernández, 1983; Martín-Merino et al., 2014).

70 The first deformation events were pre-Curavacas (prior to or earliest Moscovian) and involved the
71 emplacement of the Palentine nappes and the VU. Two generations of thrusts occurred during this episode
72 (Rodríguez Fernández, 1994), which translated sequences northwards. Further, some back thrusts and normal
73 faults occurred. Folds associated with the thrusting also formed during this episode.



74 The post-Curavacas deformation events involved the development of several generations of thrusts and
75 high-angle reverse faults, folds, cleavages and normal faults. Some thrusts have a trend approximately parallel to
76 the basal thrust of the Ponga unit and are probably related to the emplacement of this thrust unit (Rodríguez
77 Fernández and Heredia, 1987), which occurred during the late Moscovian. In the same episode that involved the
78 emplacement of the Picos de Europa thrust unit during the Kasimovian-Gzhelian (Merino-Tomé et al. 2009), N –
79 S shortening occurred in the study area, involving the development of thrusts, high angle reverse faults and the
80 reactivation of older faults with a movement dominantly southward (Maas, 1974). In addition, upright folds with
81 E – W axial trace developed; among them, the Curavacas-Lechada syncline is remarkable for its notable
82 dimensions (Savage, 1967; Lobato, 1977; Rodríguez Fernández, 1994).

83 Several cleavages have been recognised in the study area. Among them, a gently dipping cleavage
84 crosscutting folds is the most relevant and has been described by various authors (Van Veen, 1965; Savage,
85 1967; Lobato, 1977; Van der Pluijm and Kaars-Sijpesteijn, 1984; Van der Pluijm et al., 1986; Rodríguez
86 Fernández, 1994, 2001; García-López et al., 1999, 2007; Marín, 1997; Bastida et al., 2002).

87 A subsequent N-S shortening episode occurred during the Alpine deformation. It involved tightening of
88 folds, local development of crenulation cleavage and reactivation of some faults. It is responsible for the dome
89 geometry of the VU (Marín et al., 1995; Marín, 1997). Another post-Variscan structure of the study area is the
90 Ventaniella fault, which traverses the whole Cantabrian Zone in a NW – SE direction. It is essentially a dextral,
91 strike-slip fault with a net-slip of 4-5 km (Julivert et al., 1971) whose activity began in the Permian and
92 continues to the present (López-Fernández et al., 2002, 2004).

93 Outcrops of intrusive igneous rocks are common in the PCU, and their knowledge is important to
94 understand the tectonothermal evolution of this unit. Among these rocks, three granodioritic stocks (Pico Iján,
95 Peña Prieta and Pico Jano; Fig. 2) and many small outcrops can be distinguished. The latter are mainly
96 concentrated in the southern half of the unit.

97 The stocks of Pico Iján, Peña Prieta and Pico Jano dominantly have granodioritic composition and their
98 intrusion was favoured by the existence of faults (Suárez and García, 1974; Corretgé and Suárez, 1990), having
99 developed a notable aureole of contact metamorphism in the case of the Peña Prieta stock. The porphyroblasts in
100 this aureole are post-tectonic relative to the gently dipping cleavage (Gallastegui et al., 1990; Rodríguez
101 Fernández, 1994). The large number of small outcrops of igneous rocks that exist in the southern half of the unit
102 are concentrated in two areas (one in the eastern part and another in the western part) joined by a band whose
103 outcrops of igneous rocks have been related to the León fault (Corretgé et al., 1987; Suárez and Corretgé, 1987;
104 Corretgé and Suárez, 1990). All these southern outcrops have been in general related to fractures and appear as
105 small stocks, probably apophyses of bigger bodies in depth, and as sills or dikes. Their composition is varied and
106 ranges from granodioritic to gabbroic. In some cases, they developed ore bodies close to their contacts (Martín-
107 Izard et al., 1986).

108 Earlier metamorphic studies in the Cantabrian zone using CAI and/or KI methods have shown the existence
109 of areas with very low- or low-grade metamorphism in the PCU and the VU (Raven and van der Pluijm, 1986;
110 Keller and Krumm, 1993; Marín et al., 1996; Marín, 1997; Köberle et al., 1998; García-López et al., 1999, 2007,
111 2013; Bastida et al., 2002; Clauer and Weh, 2014; among others). Similar results have been obtained for the
112 southern part of the study area using coal rank and vitrinite reflectance (Colmenero and Prado, 1993; Llorens et
113 al., 2006; Colmenero et al., 2008; Clauer and Weh, 2014). This metamorphism has been described as associated



114 with a late-orogenic extensional event and to the corresponding cleavage (García-López et al., 1999, 2007, 2013;
115 Bastida et al., 2002). Analysis of ore deposits and of the tectonothermal evolution in the neighbouring unit of the
116 Picos de Europa has defined a subsequent hydrothermal episode during the Permian (Gómez-Fernández et al.,
117 1993, 2000; Bastida et al., 2004). Brime and Valín (2006) have suggested a hydrothermal origin for mineral
118 associations with chloritoid and pyrophyllite found in samples of pelitic rocks collected in the study area. K-Ar
119 dating of illite in samples collected in the southern part of the study area, identified four thermal episodes (Clauer
120 and Weh 2014), namely at: (1) 293 ± 3 Ma (Cisuralian), (2) 268 ± 6 Ma (Guadalupian), (3) 243 ± 5 Ma (middle
121 Triassic), and (4) 175 ± 6 Ma (early-middle Jurassic). From apatite fission tracks and zircon (U-Th)/He ages in
122 samples of Westphalian (Bashkirian-Moscovian) sandstones collected in the eastern part of the PCU, Fillon et al.
123 (2012) obtained ages of cooling below $\approx 180^\circ\text{C}$ of 37-39 Ma and below $\approx 110^\circ\text{C}$ of 28-29 Ma. They inferred
124 Cenozoic erosion of a rock thickness between 6.4 and 8 km (assuming a steady-state geothermal gradient of
125 25°C km^{-1}).

126 3 Methods

127 3.1 X-ray diffraction

128 A total of 297 mudrocks from various localities (Fig. 2) were studied by X-ray diffraction (XRD) analysis in
129 order to determine their phyllosilicate mineralogy, Kübler Index (KI) of illites, and Árkai Index of chlorites (AI).
130 Preparation of samples and methods for XRD analysis follow the methods described in Brime et al. (2003)

131 Reaction progress in illitic minerals (*sensu* Środoń 1984) has been widely used to assess the evolution of
132 pelitic lithologies during diagenesis and low-grade metamorphism. Prograde changes can be identified by use of
133 the Kübler Index technique (illite “crystallinity”, see Guggenheim et al. 2002) involving quantification of the
134 width of the 10Å peak of illite. This is an indirect measure of lattice reorganization and thickening of illite
135 crystals (Kisch 1983; Merriman and Peacor 1999) with increasing grade. The Kübler Index (KI) is expressed in
136 $\Delta^\circ 2\theta$ to minimize variations caused by differences in recording conditions. For this study the KI was measured
137 using a laboratory procedure similar to that outlined by the IGCP 294 working group (Kisch, 1991). The
138 numerical KI value decreases with improving “crystallinity” and is expressed as small changes in the Bragg
139 angle $\Delta^\circ 2\theta$, using Cu K α radiation.

140 The transient zone between diagenesis and metamorphism (the anchizone of Kübler, 1967) is defined by KI
141 values between 0.42° and $0.25^\circ \Delta^\circ 2\theta$ respectively (Kisch, 1991). The values obtained in our laboratory were
142 correlated with the Kübler scale using a calibration curve based on data obtained from polished slate standards
143 kindly provided by H. Kisch. The diagenetic zone has been subdivided in shallow ($\text{KI} > 1^\circ \Delta^\circ 2\theta$) and deep (1.0°
144 $> \text{KI} > 0.42^\circ \Delta^\circ 2\theta$), using the terms proposed by the IUGS Subcommittee on the Systematics of Metamorphic
145 rocks (Árkai et al., 2007). Following Merriman and Peacor (1999) we have divided the anchizone into low (0.42
146 $< \text{KI} < 0.30^\circ \Delta^\circ 2\theta$) and high ($0.30 < \text{KI} < 0.25^\circ \Delta^\circ 2\theta$).

147 Crystallinity index standards (CIS, Warr and Rice 1994) have also been used to compare the results thus
148 obtained with other published results using that scale. KI values obtained in this work could be converted to the
149 CIS scale by using the calibration equation:

$$150 \text{KI}_{\text{CIS}} = 1.505\text{KI}_{\text{this work}} - 0.046 \quad (R^2 = 0.996). \quad (1)$$



151 For the problems involved in the use of the CIS scale to assess metamorphic grade see Brime (1999) and
152 Kisch et al. (2005).

153 The KI method does not allow temperature constraints to be placed on the upper and lower boundaries of
154 the anchizone and it is more likely to be a measure of reaction progress than of the thermodynamic equilibrium
155 achieved (Essene and Peacor, 1995). However, this method, in combination with others such as fluid inclusions
156 or reflectance of carbonaceous material, indicates that the transition diagenesis–anchizone could be correlated
157 with a temperature of 230 ± 10 °C whereas the limit anchizone–epizone would be at 300 ± 10 °C (Müllis, 1979;
158 Frey et al., 1980; Frey, 1987; Von Gosen et al., 1991; Müllis et al., 1995; Merriman and Frey, 1999; Ferreiro
159 Mählmann et al. 2002; Müllis et al. 2002).

160 The presence of illite/smectite (I/S) and paragonite (Pg) and paragonite/muscovite (Pg/Ms) hampers
161 determination of KI of many samples. However, pro-grade changes can also be identified by use of the Árkai
162 Index technique (of chlorite “crystallinity”, see Guggenheim et al., 2002) involving quantification of the width of
163 the 14Å or 7Å peaks of chlorite (Árkai, 1991, Meunier, 2005). The Árkai Index (AI) was determined in the (002)
164 peak using the same instrumental conditions as that for KI measurements. The anchizone limits have been
165 established using samples free of I/S, Pg-Pg/Ms in which the KI measured in the air dried samples has been
166 calibrated with Kisch standards. The AI was measured in the same samples and the regression line obtained
167 allowed the delimitation of the upper and lower anchizone limits using chlorite for AI values of 0.234 and 0.135
168 $\Delta^2\theta$ respectively. It should be noted that AI values are smaller than the corresponding KI and the method is
169 therefore slightly less sensitive than KI method.

170 3.2 Conodont colour alteration index (CAI).

171 Colour changes in conodont elements are related to the progressive and irreversible alteration of the amounts of
172 organic matter within their apatite composition. The CAI method is based on analysis of the colour changes that
173 the conodonts undergo in response of the organic matter to a temperature increase with time. These changes
174 permit construction of a scale of CAI values with eight units that allows the use of the conodonts as maximum
175 paleothermometers for a temperature interval of between 50 and 600°C (Epstein et al., 1977; Rejebian et al.,
176 1987). It is used mainly in carbonate rocks. Besides colour changes, apatite textural alteration also takes place
177 and can provide complementary information about the thermal conditions. In the present paper the terminology
178 of Rejebian et al. (1987) and García-López et al. (1997, 2006) is used for the textural description of conodonts.
179 In agreement with Rejebian et al. (1987), well preserved conodonts and high CAI values with a wide dispersion
180 are indicative of contact metamorphism. Furthermore, coarse recrystallization and corrosion are related to
181 hydrothermal processes.

182 Samples were collected from the Pisuerga-Carrión and Valsurbio units. CAI values are based on 5 kg
183 samples of limestone that were treated, with 6% acetic acid solution. Unfortunately, recovery of conodonts from
184 Carboniferous rocks was hindered in some areas by their dominantly siliciclastic character. Sampling was
185 complemented with specimens from collections housed at the University of Oviedo (Spain) and those of the
186 National Museum of Natural History at Leiden (Netherlands) and Institut und Museum für Geologie und
187 Paläontologie in Göttingen (Germany) (Fig. 2). 213 positive samples, corresponding to an age interval from the
188 Pridoli to Ghzelian, were analyzed for CAI determination (Appendix 1 in the supplementary material).



189 The methodology involved in CAI determination can be found in García-López et al. (1997) and Bastida et
190 al. (1999). Several CAI values were obtained from most samples and the mean of CAI values have been
191 determined for each of them in order to tentatively contour CAI values. Samples with a range higher than 1.5
192 have not been used to obtain mean CAI values and temperatures. The interpretation of the results is mainly based
193 on the analysis of the CAI isograds and their relationship to the stratigraphic contacts and the main structures of
194 the study area.

195 For the metamorphic zonation from CAI data, we use the terminology described by García-López et al.
196 (2001), that involves a division in diacaizone ($CAI < 4$), ancaizone ($4 \leq CAI \leq 5.5$) and epicaizone ($CAI > 5.5$).

197 Temperature ranges of the CAI values were obtained from the Arrhenius plot presented by Epstein et al.
198 (1977) and Rejebian et al. (1987). The maximum heating time is the age of the rock. Nevertheless, it is possible
199 to place greater limits on this maximum time (García-López et al., 2013). According to the Arrhenius plot a
200 minimum temperature is required to obtain a specific CAI value. For example, in a rock with an age of 400 Ma
201 (Devonian), development of $CAI = 5$ requires at least 290°C (point A in Fig. 3). Then, it can be assumed that a
202 temperature $< 290^{\circ}\text{C}$ does not contribute to generate a $CAI = 5$. Hence, to produce a given CAI, the maximum
203 time of heating begins when the rock reaches the minimum temperature necessary to produce that CAI, and it
204 ends when the rock cools down and the temperature becomes lower than this minimum value. According to
205 García-López et al. (2013), and in agreement with the age of the metamorphism analyzed below, we consider
206 that the main heating time corresponds to a late-Variscan period that began at the boundary Kasimovian-
207 Gzhelian and ended at the beginning of the Triassic (heating time of about 50 Ma). The hydrothermal post-
208 Variscan episodes described by Clauer and Weh (2014) and the most recent heating (mainly Cenozoic) described
209 by Fillon et al. (2012) probably lasted less than 50 Ma. If there are rocks within the area that underwent more
210 than one heating period, the period to be considered for the development of the CAI is the one which generated
211 higher temperatures. Anyway, due to the geometry of the CAI curves in the Arrhenius plot, for heating intervals
212 such as those involved in the present case, an error of a few Ma in the maximum time of heating has little
213 influence on the results. According to Patrick et al. (1985) and Rejebian et al. (1987) the minimum time of
214 heating assumed here is of 1 Ma.

215 3.3 Cleavage

216 Development of cleavage requires ductile deformation of rocks and mineralogical and microstructural changes,
217 involving mechanisms, such as pressure solution, which require a minimum temperature of about 200°C for
218 cleavage development in pelitic rocks and 175°C in limestones (Groshong et al. 1984). Thus widespread
219 presence of cleavage occurs below a certain crustal level (minimum overburden of 5-7 km; Engelder and
220 Marshak, 1985). Furthermore, the relations between folds and cleavages and the overprinting relations between
221 cleavages, play an important role in defining deformation events (Passchier and Trouw, 2005). In addition,
222 cleavage is also a key structure to establish chronological relations between metamorphic crystallization and
223 deformation. In the context of the study area, we call tectonothermal event to a deformational event with
224 cleavage development and associated metamorphic conditions, and use the term thermal event for metamorphic
225 conditions without cleavage development. Hence, cleavage is considered here as the main reference to ascertain
226 the tectonothermal events of the study area.

227 4 Results and interpretation

228 In order to facilitate description, the samples have been grouped in the following areas, namely Liébana,
 229 Valdeón, Yuso-Carrión, Pisuerga, Riaño-Cervera and Valsurbio (Fig. 4) (cf. Martín-Merino et al., 2014).

230 4.1 Clay minerals

231 4.1.1 Clay mineral assemblages

232 Mineralogical analysis of the <2 μm fractions shows that dioctahedral K- rich mica-like structures (referred to as
 233 illite or muscovite, I-Ms) is present in all the samples with the majority containing also chlorite (Chl) (Fig. 5).
 234 Chlorites have poorly developed 14 Å peaks, indicating high iron content suggestive of chamositic compositions
 235 (Moore and Reynolds, 1997). Other phases such as ordered illite/smectite (I/S) or paragonite (Pg) and mixed
 236 layers paragonite/muscovite (Pg/Ms) are also common. Asymmetry of peaks and sample behaviour after
 237 glycolation indicate the presence of ordered illite/smectite (I/S). Absence of random I/S indicate that zone 3 of
 238 Eberl (1993) has been reached, suggesting that temperatures exceeded 100°C. Kaolinite (Kln) and pyrophyllite
 239 (PrI) may also be present in some samples and are abundant in a few samples. In addition, chloritoid (Cld) is also
 240 present and widespread in the study area. However it is more abundant in samples close to the intrusions and/or
 241 faults in which case is found together with chlorite and Pg + Pg/Ms. Only in samples to the E (Pisuerga Area),
 242 where it is not as abundant, it may be associated with PrI, Kln or I/S. Finally chlorite/vermiculite mixed
 243 layer (C/V) and stilpnomelane (Stp) have been found, in small amounts, in a few samples, and are restricted to
 244 samples to the E Pisuerga and E Yuso-Carrión areas.

245 The I/S is more abundant to the N and E (Valdeón, Liebana, and eastern part of the Pisuerga and Yuso-
 246 Carrión areas) and Kln presence is almost restricted to samples to the E (Pisuerga and eastern part of the Yuso-
 247 Carrión areas). PrI is common in samples from the central and northeastern parts (Liebana and Pisuerga areas,
 248 and eastern part of the Yuso Carrión area) (Fig. 5). Quartz, calcite, feldspars and goethite were accessory phases
 249 recognized in some samples.

250 In general the assemblages found are, in order of abundance of the most frequent phase besides illite (n =
 251 291):

252 I + **Chl** (n = 215) ± Pg ± Pg/Ms ± Cld ± I/S ± [C/V] ± [PrI] ± [Kln] ± [Stp]

253 I + **Pg + Pg/Ms** (n = 162) ± Chl ± Cld ± [I/S] ± [PrI] ± [C/V] ± [Kln] ± [Stp]

254 I + **I/S** (n = 112) ± Chl ± Kln ± PrI ± C/V ± Pg ± Pg/Ms ± C/V ± [Cld] ± [Stp]

255 I + **Cld** (n = 93) ± Chl ± Pg ± Pg/Ms ± I/S ± [C/V] ± [PrI] ± [Kln] ± [Stp]

256 I + **PrI** (n = 56) ± I/S ± Chl ± Pg ± Pg/Ms ± C/V ± [Cld] ± [Kln] ± [Stp]

257 I + **C/V** (n = 48) ± I/S ± Chl ± Pg ± Pg/Ms ± Kln ± PrI ± Cld ± [Stp]

258 I + **Kln** (n = 39) ± I/S ± Chl ± C/V ± [PrI] ± [Cld] ± [Pg] ± [Pg/Ms] ± [Stp]

259 4.1.2 Kübler Index

260 As mentioned above, determination of KI has been hampered by the presence in some samples of certain types
 261 of I/S and big amounts of Pg or PrI, in relation to the amount of illite, that interfere with the 001 peak of illite,



262 therefore rendering their KI values useless for grade determination using KI, even in the glycolated state. As a
263 result, 23 (indicated in *italics* in Appendix 2 in the supplementary material) of the 291 samples studied yielded
264 doubtful KI values (Figs. 6, 7; Appendix 2 in the supplementary material). They are given, nevertheless, as they
265 indicate maximum value of the KI.

266 Grade ranges from deep diagenetic to epizonal, but deep diagenetic and mainly low anchizonal metapelites
267 are predominant in most of the areas (Figs. 6 and 7). Expandability of the 10 Å peak is only lost at the high
268 anchizone to epizone boundary. Deep diagenetic areas can be found to the north (Liébana and Valdeón areas).
269 The Riaño-Cervera area is mainly low anchizonal with a few samples being diagenetic or deep anchizonal. In the
270 Pisuega area, the grade ranges from deep diagenetic to low anchizonal (Figs. 6, 7). Higher grade (epizonal)
271 samples may appear in any formation and they are more abundant in the western part of the Yuso-Carrión area,
272 where a big size intrusion is located, and in the Devonian of the Valsurbio area (Fig.7). In both cases, it is in
273 those high grade samples where chloritoid is more abundant (Fig.6).

274 Work in progress on the variation of the chemical composition of the phyllosilicates of the study area
275 allowed estimation of temperatures using Battaglia's (2004) approach based in the variation in the chemical
276 composition of illites. Temperatures obtained are in the range 230-280°C, consistent with the anchizonal KI
277 values of the analyzed samples. The observed deficit in layer charge (Brime and Valín, 2006) is characteristic of
278 anchizonal K white micas (Hunziker et al 1986; Livi et al. 1997; Merriman and Peacor 1999; Árkai 2002; Árkai
279 et al 2003).

280 4.1.3 Árkai Index

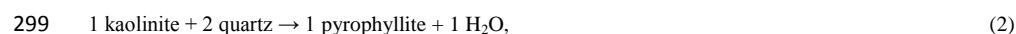
281 It has been measured in 118 samples, most if not all of them, containing various amounts of I/S and/or Pg,
282 Pg/Ms. Of them, 40 yielded diagenetic values, 63 low anchizonal values, 14 high anchizonal values and just one
283 epizonal value. Distribution of these values can be seen in Fig. 6. In those cases in which KI and AI have been
284 determined, the correlation of the grade indicated by both indices is good ($r = 0.65$; significance level 0.1% $r_{60} =$
285 0.41) suggesting that both phases were formed under the same conditions, and supporting the reliability of the AI
286 as indicator of grade in those cases in which it is the only index available (Árkai et al., 1995).

287 The existence of some discrepancies between KI and AI may be caused by the presence of small amounts
288 of I/S or Pg that alters the width of the illite peaks. However, those discrepancies are always small and are
289 usually in samples at the boundary between metamorphic grade zones (Appendix 2 in the supplementary
290 material).

291 4.1.4 Mineral distribution in relation with grade

292 Kaolinite is present in deep diagenetic samples and also in some low anchizonal ones. Maximum stability of Kln
293 is 270°C, according to laboratory experiments (Velde, 1992) and therefore in agreement with its presence in the
294 anchizonal samples. Paragonite, apart from its presence in deep diagenetic samples, is more frequently present in
295 the anchizone and some epizonal samples (Figs. 5 and 6). Pyrophyllite is more abundant in samples from the
296 anchizone but it can also be present in diagenetic samples.

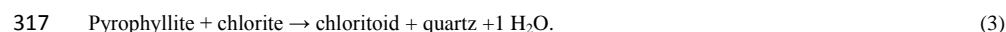
297 The widespread occurrence of Kln and quartz in the diagenetic rock samples may provide the starting
298 material for the formation of Prl by the reaction





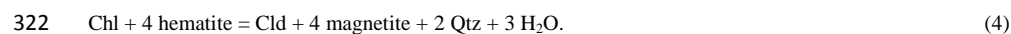
300 as suggested in the Glarus Alps by Frey (1978), who considered Prl an indicator of anchizone regional
301 conditions. In fact of the 53 samples in which Prl is present, Kln is found, and in very small amounts, in only 8
302 of them. However, the stability field of Prl is strongly influenced by water activity, and thus the formation
303 temperature could be notably lower (Thompson, 1970; Winkler, 1979; Hemley et al., 1980). Its presence in
304 diagenetic samples is not uncommon and could be due to the influence of magmatic fluids (Hosterman et al., 1970;
305 Kisch, 1987). According to Kisch (1987) Prl, appears in regional terrains only in the anchizone but in areas of
306 intrusive activity it may appear in lower grade zones. Therefore presence of Prl in samples with diagenetic KI/AI
307 values, as in the eastern part of the Liebana and Yuso Carrión areas, could be regarded as evidence for high
308 geothermal gradients or magmatic heating.

309 Chloritoid is abundant in samples from the high anchizone to epizone (southeastern Valsurbio area and
310 western Yuso Carrión area), but it can also be present, in smaller amounts, in low anchizone (1, 3W, 4E, 4W,
311 5E, 5W) and even diagenetic samples (eastern Liébana, Pisuerga and Riaño-Cervera areas). Cld is Fe rich. The
312 average $Mg/(Fe+Mg)$ found is < 0.12 (Brime and Valín, 2006) similar to that of pelites subjected to intermediate
313 P/T conditions. It is noteworthy that when this phase is present in the samples (a total of 93 samples have Cld),
314 Prl is absent, or in very minor amounts in a few samples (ten in total), indicating that it could have been formed
315 according to the reaction originally proposed by Zen (1960), which is generally accepted for the formation of
316 Cld during metamorphism of aluminous pelites (Theye et al. 1992):

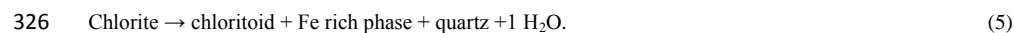


318 The absence of Cld in the eastern part of the Yuso Carrión area where Prl is abundant, together with Chl,
319 could indicate that the temperature required for its formation by reaction (3) has not been reached.

320 Presence of some Fe oxides has been detected in samples from the study area. Therefore more Cld could be
321 produced by the reaction suggested by Bucher and Frey (1994):



323 However, it has been observed in thin sections that occurrence of Prl is almost restricted to veins and
324 fracture zones, suggesting that Cld could have been formed during the hydrothermal alteration of the pelites
325 following the reaction proposed by Phillips (1988):



327 Presence of Cld in the anchizone has been discussed by Kisch (1983), who concluded that Cld cannot
328 unequivocally be regarded as an indicator of the beginning of the epizone, as previously suggested, because there
329 are occurrences in the anchizone (Árkai et al., 1981). In the study area, Cld is more abundant in the epizone
330 samples of the Valsurbio (6) and W Yuso-Carrion (3W) areas, but it is also present in low anchizone and a few
331 deep diagenetic samples from the Riaño Cervera (5E), Pisuerga (4E) or Valdeón (2) areas, thus corroborating the
332 conclusion of Kisch (1983).

333 Chloritoid and Prl are widespread in virtually all rock types and grade conditions (Appendix 2 in the
334 supplementary material). This occurrence could be related to basin wide alteration by infiltrating hydrothermal
335 fluids (Phillips, 1988; Brime and Valín, 2006). Late to post Variscan fluid flow events have been described in the
336 other areas of the Cantabrian Zone (Ayllón et al., 2003; Gasparri et al., 2003) and related to a more general
337 Variscan event (Boni et al., 2000).



338 4.2 Conodont colour alteration index (CAI).

339 The CAI values are independent of the stratigraphic position of the samples (Fig. 8). These values vary widely,
340 ranging from 1.5 to 7.5, corresponding respectively to intervals of temperatures of < 40-60°C and 550-590°C
341 (see Appendix 1 in the supplementary material). However, values equal to or lower than 2 are unusual, being
342 limited to the southeastern sector of the Pisuerga-Carrión unit. Some samples with conodonts having high CAI
343 values and a range of one and a half units, or more, are indicative of contact metamorphism and/or hydrothermal
344 processes. Values ≥ 6 are usually found close to outcrops of igneous rocks. The upper boundary of the ancaizone
345 (CAI = 4) corresponds to a temperature range of 190 - 225°C, while the lower limit (CAI = 5.5) corresponds to
346 the range of 340-375°C.

347 The lack of carbonate rocks prevents in some areas the construction of a complete map of CAI isograds;
348 however, it is possible to observe that they crosscut the trend of the Variscan structures. CAI data allow the
349 distinguishing of the following sectors in the study area (Fig. 8):

- 350 (a) Northern sector (Liebana and Valdeón areas). This is an ancaizonal area that passes without thermal
351 discontinuity through the basal thrust of the Picos de Europa unit. Inside this unit, the boundary
352 ancaizone/diacaizone appears and the CAI decreases northwards (Bastida et al., 2004; Blanco-Ferrera et al.,
353 2011).
- 354 (b) Central-eastern sector (eastern part of the Yuso-Carrión area) with dominance of ancaizonal conditions. Here,
355 in the areas where CAI data exist, a remarkable homogeneity of CAI values appears, mainly in the Devonian
356 rocks of the area located to the east of the Curavacas-Lechada syncline.
- 357 (c) Central and western sectors, (western part of the Yuso-Carrión and Riaño-Cervera areas) where the limited
358 CAI data available indicate that epicaizonal areas coexist with ancaizonal areas.
- 359 (d) Southern sector. It corresponds to the VU and presents a wide area with epicaizonal conditions (García-
360 López et al., 2013).
- 361 (e) Southeastern sector (eastern part of the Yuso-Carrión and Pisuerga areas). In this area, diacaizonal
362 conditions are dominant, but ancaizonal and epicaizonal areas also appear. The latter areas appear adjacent
363 to outcrops of igneous rocks. The greater variation of CAI values is found in this area, with a range from 1.5
364 to 7.

365 The apparently chaotic distribution of CAI isograds is probably due to a heat from subsurface intrusions at
366 depth resulting in isotherms having complex geometry. This pattern may be related to a crustal thinning during
367 an extensional episode and to the subsequent intrusion of igneous bodies that emplaced at different levels,
368 generating contact metamorphism and hydrothermal fluids.

369 In general, conodonts of the study area are undeformed and well preserved. Most of them have granular
370 texture due to apatite recrystallization under high temperature. The apatite crystals do not show preferential
371 orientation and their size increases with the temperature. The granular texture is commonly incipient for CAI
372 values between 4 and 4.5 and is widespread for CAI values ≥ 5 . Furthermore some conodonts with CAI values
373 between 6 and 7 have coarse recrystallization, corrosion and loss of ornamentation, so that in a few cases they
374 have lost their original morphology (“ghost conodonts”). These alterations of conodonts with CAI values ≥ 5 are
375 indicative of contact metamorphism and hydrothermal processes. Some conodonts with CAI ≥ 4.5 present sets of
376 parallel microfissures, probably related to the rock cleavage. Conodonts with CAI ≤ 4 have occasionally
377 unaltered surfaces, but most of them present a sugary texture (dull, frosted or pitted surfaces). The surfaces of

378 these conodonts show several types of overgrowth of apatite crystals, mainly developed independently of the
379 CAI value (or thermal changes under diacaizonal conditions); they were usually a result of apatite solution and
380 crystallization processes (Blanco-Ferrera et al., 2011).

381 **4.3 Cleavage development and tectonothermal events**

382 Two main cleavages have been found in the study area (Fig. 9). Cleavage S_1 is a rough foliation associated with
383 upright folds and trends approximately E-W; it appears mainly in the northern half of the study area. This
384 cleavage affects latest Carboniferous rocks (Kasimovian-Gzhelian age). Cleavage S_2 dips gently, crosscuts
385 earlier upright folds and is associated with the development of meter-scale open cascade folds. It is especially
386 well developed in the Curavacas-Lechada syncline and in the VU. Both cleavages appear in different areas and
387 have not been observed superimposed. The existence of two cleavages with different age suggests that two
388 tectonothermal events took place in the southeastern sector of the CZ.

389 The first event, associated with the S_1 cleavage (sub-vertical), is not well defined, since it developed in an
390 area where presence of I/S and Kln and KI and AI values indicate deep diagenesis or low anchizonal conditions,
391 and CAI values dominantly show ancaizonal conditions. According to the age of the latest rocks affected, this
392 event probably occurred during the late Gzhelian. It resulted in crustal thickening produced by the N - S
393 shortening that gave rise to the emplacement of the Picos de Europa unit, the last major Variscan thrust unit that
394 was generated in the foreland fold and thrust belt, and it disassociated with the development of other thrusts and
395 folds to the south of this unit.

396 The second event produced cleavage S_2 that crosscuts the upright folds in the southern part of the study
397 area (Curavacas-Lechada syncline and the VU). Under the microscope, this cleavage shows evidences of
398 pressure solution and crystallization of oriented muscovite and chlorite with formation of chlorite-muscovite
399 porphyroblasts. X-ray diffraction indicates that the rocks affected by this cleavage present Chl + Pg-Pg/Ms
400 assemblages; KI and AI values indicate high anchizonal to epizonal conditions and CAI values indicate similar
401 conditions. The gently dipping attitude of S_2 suggests that this event was associated with an extensional
402 deformation and the corresponding crustal thinning as a consequence of a late orogenic gravitational
403 readjustment of the orogen in the core of the Ibero-Armorican arc. This interpretation agrees with the kinematic
404 evolution of the arc proposed by Gutiérrez-Alonso et al. (2004, 2011). The event culminated with the intrusion
405 of igneous rocks that traversed the rocks with cleavage and generated a contact metamorphism associated with
406 hydrothermal processes, as indicated by: (1) the widespread presence of Cld and Prl (Fig 5; Brime and Valín,
407 2006) and low KI and AI values, (2) recrystallization in conodonts (granular texture), (3) high CAI values in
408 samples close to outcrops of intrusive rocks, (4) wide range of CAI in some samples, and (5) irregular variation
409 of the CAI through the area and strong corrosion in some conodonts. The cleavage S_2 developed earlier than the
410 porphyroblasts (biotite, andalusite and chloritoid) formed during the contact metamorphism associated with the
411 granodioritic stock of Peña Prieta (Gallastegui et al., 1990; Rodríguez Fernández, 1994), whose age is Ciszuralian
412 (292+2/-3 Ma after Valverde-Vaquero et al., 1999). These data suggest the development of a thermal event that
413 took place near the boundary Carboniferous-Permian and that progressed during the Ciszuralian with the intrusion
414 of many small igneous bodies that rose along faults (Suárez and García, 1974; Corretgé and Suárez, 1990).

415 In some locations, S_2 is gently folded with local development of crenulation cleavage. This may be a result
416 of the Alpine deformation, which is the only post-Variscan compressional deformation described in the area

417 (Gallastegui, 2000 and references therein), and involves a ductile deformation that required a moderate
418 temperature and gave rise to a dome shape in the Valsurbio unit (Marín, 1997).

419 The features described above refer to late-Variscan events related to the development of penetrative
420 structures or to the intrusion of igneous rocks. However, the existence of such events does not preclude the
421 development of others subsequently, such as the hydrothermal post-Variscan episodes described by Boni et al.
422 (2000), Muchez et al. (2005), Gasparrini et al. (2006) and Clauer and Weh (2014).

423 5 Discussion

424 The distribution of the different grade indicators used in the study area shows, in general, an acceptable
425 correlation between them, although some discrepancies have been observed. All methods coincide in pointing
426 out the location of the areas with higher metamorphic grade, being the CAI and the AI the indicators that tend to
427 give the highest and the lowest grade respectively. All indices point to an irregular distribution of the areas with
428 very low-grade metamorphism. Diacaizonal areas are limited to the southeastern sector. A discrepancy is
429 observed in the eastern Yuso-Carrión area between clay mineral and CAI data. A notable number of CAI values
430 systematically indicate ancaizonal conditions, whereas clay assemblages with abundant I/S and Kln, KI and AI
431 indicate diagenetic conditions.

432 The correlation among the different indicators that can be used to establish the metamorphic grade is
433 challenging due to several factors, such as the different kinetics of the processes that modify the colour of the
434 conodonts and the transformation of the clay minerals and the different influence of fluids in limestones and
435 pelitic rocks. These processes could explain the discrepancies observed.

436 In the context of the Cantabrian Zone, the low-grade extensional metamorphism of the PCU extends
437 westwards and allows an elongated area to be defined that can be followed up to the Central Coal Basin (Fig. 1)
438 (Aller, 1981, 1986; Brime, 1985; Aller et al., 1987, 2005; García-López et al., 2007). The biggest width of this
439 zone is in the study area, coinciding with the core of the Ibero-Armorican arc. In the Central Coal Basin, this
440 metamorphism is linked to the occurrence of cleavage associated with crosscutting folds and it has been related
441 to the possible existence of igneous bodies in depth (Aller, 1986) or to the rise of fluids along faults, especially
442 the León fault (Aller et al., 2005). In the metamorphic southern part of the study area (VU), the metamorphism
443 disappears westward, so that the adjacent western unit of the Esla nappe region is not metamorphic (García-
444 López et al., 2013; Valín and Brime unpublished data).

445 The existence of hydrothermal alteration has been suggested by Brime and Valín (2006) and Clauer and
446 Weh (2014). The common occurrence of Cl₂ and Pr₁ and the irregular distribution of CAI values, the wide range
447 in the high CAI values in some samples and textural alterations of conodonts agree with the occurrence of
448 hydrothermal fluids and possible subsurface igneous bodies. As for the thermal events dated by Clauer and Weh
449 (illite K-Ar; 2014), the first has an age(293 ±3 Ma), comparable to that of the Peña Prieta granitoid (292+2/-3 Ma
450 after Valverde-Vaquero et al., 1999, Cisuralian), and the others (Guadalupian, middle Triassic and early-middle
451 Jurassic) are probably related to the crustal extension associated with the Basque-Cantabrian basin. Specific
452 structural evidences of these three later events have not been found and their temperatures were probably lower
453 than those of the episode linked to the late-Variscan extensional episode, which, being related to igneous
454 intrusions, probably gave rise to the paleothermal peak.

455 The zircon (U-Th)/He ages obtained by Fillon et al. (2012) indicate that the Westphalian (Bashkirian-
456 Moscovian) rocks involved in the dating had probably a temperature above 180°C up to 37-39 Ma ago (Eocene).
457 This is consistent with the occurrence of Alpine ductile deformation, which resulted in a local crenulation
458 cleavage.

459 6 Conclusions

460 Study of the low-grade metamorphic rocks and associated structures in the south-eastern sector of the CZ has
461 allowed a model for the tectonothermal evolution of the core of an arcuate orogenic belt to be developed. This
462 core, although it is a part of a foreland fold and thrust belt where diagenetic conditions are dominant, portrays a
463 complex evolution due to its special location inside the belt. It was thrust during the Carboniferous by large units
464 from south, west and north, which resulted in a great accumulation of syntectonic sediments, and development of
465 unconformities and structures. The latter arose as a result of compression in different directions that also
466 generated a crustal thickening. The emplacement of the last thrust unit (Picos de Europa unit) produced a N – S
467 shortening that generated thrusts and associated folds. Shortly afterwards, upright folds with E – W trend and
468 associated cleavage (S_1) developed, mainly in the northern part of the sector. The ductile deformation occurred
469 under thermal conditions which reached the anchizone and the ancaizone in some areas. This represents the first
470 tectonothermal event registered in the southeastern sector of the CZ.

471 At the end of the Variscan deformation, gravitational instability gave rise to an extensional episode and the
472 corresponding crustal thinning. During this event an increase in the thermal gradient enabled ductile deformation
473 and low-grade metamorphism to take place in some areas (second tectonothermal event), mainly in the central
474 part (Curavacas-Lechada syncline) and the southern part (Valsurbio unit) of the sector. The ductile deformation
475 produced gently dipping cleavage (S_2) crosscutting earlier upright F_1 folds. Some small open cascade folds were
476 also produced. The metamorphism reached epizonal and epicaizonal conditions during this event. The process
477 culminated in the Cisuralian with the intrusion of igneous rocks and the development of contact metamorphism
478 around the larger igneous bodies. In the case of Peña Prieta granodiorite, post S_1 andalusite porphyroblasts
479 developed. Hydrothermal fluids were common during this extensional episode, resulting in the development of
480 Prl and Cld , and textural alteration and high CAI dispersions in conodont samples.

481 As a whole, the metamorphic grade is independent of the stratigraphic location of the samples and the trend
482 of the main structures, indicating the late-orogenic character of the tectonothermal events. The thermal level
483 decreases progressively northwards inside the adjacent Picos de Europa unit. On the other hand, the
484 metamorphism associated with the extensional episode in the PCU is extended westwards as an elongated area
485 whose development was probably favoured by the rise of fluids along faults, especially along the León fault.

486 With the development of the adjacent Basque-Cantabrian basin, the extensional regime extended during the
487 Mesozoic, with the probable occurrence of hydrothermal processes. The temperature of the rocks was probably
488 important during Cenozoic times (> 180°C until the late-Eocene after Fillon et al., 2012, in the eastern part of the
489 study area), so that the Alpine deformation generated locally some ductile deformation with crenulation cleavage
490 affecting the S_2 cleavage.

491 The evolution described above is summarized in Table 1.

492

493 **Acknowledgements.** This paper is dedicated to the memory of Andrés Pérez Estaún in recognition to his major
494 contribution to the study the geology of the Variscan belt in Spain and his pioneer work on the low-grade
495 metamorphism of the area, and in gratitude for fruitful cooperation over a period of many years. The present
496 paper has been supported by the CGL2015-66997-R project funded by the Spanish Ministry of Economy and
497 Competitiveness. The authors acknowledge Dr. Robin Offler who read an earlier version of this paper and
498 suggested improvements. Susana García-López acknowledges the cooperation of C. F. Winkler Prins from the
499 National Museum of Natural History (Leiden, Netherlands) and H. Jahnke from the Institut und Museum für
500 Geologie und Paläontologie (Göttingen, Germany) in facilitating access to the Cantabrian conodont collections
501 of these institutions.

502 **References**

- 503 Aller, J.: La estructura del borde sudoeste de la Cuenca Carbonífera Central (Zona Cantábrica, NW de España),
504 *Trabajos de Geología*, 11, 3-14, 1981.
- 505 Aller, J.: La estructura del sector meridional de las unidades del Aramo y Cuenca Carbonífera Central,
506 *Principado de Asturias, Spain*, 180 pp, 1986.
- 507 Aller, J., Bastida, B., Brime, C., and Pérez-Estaún, A.: Cleavage and its relation with metamorphic grade in the
508 Cantabrian Zone (Hercynian of North-West Spain), *Sci. Géol. Bull.*, 40, 255-272, 1987.
- 509 Aller, J., Valín, M.L., García-López, S., Brime, C., and Bastida, F.: Superposition of tectono-thermal episodes in
510 the southern Cantabrian Zone (foreland thrust and fold belt of the Iberian Variscides, NW Spain), *Bull. Soc.
511 Géol. France*, 176, 503-514, 2005.
- 512 Alonso, J.L. and Rodríguez Fernández, L.R.: Las discordancias carboníferas de la región del Pisuerga-Carrión
513 (Cordillera Cantábrica, NO de España). Significado orogénico, *Comptes Rendus del X Congreso
514 Internacional de Estratigrafía y Geología del Carbonífero*, Instituto Geológico y Minero de España, Madrid,
515 Spain, 533-540, 1983.
- 516 Alonso, J. L., Marcos, A., and Suárez, A.: Paleogeographic inversion resulting from large out of sequence
517 breaching thrusts: The león Fault (Cantabrian Zone, NW Iberia). A new picture of the external Variscan
518 Thrust belt in the Ibero-Armorican Arc, *Geologica Acta*, 7, 451-473, doi: 10.1344/105.000001449, 2009.
- 519 Alonso, J. L., Marcos, A., and Suárez, A.: El Cabalgamiento de León: implicaciones en la división geológica de
520 la Zona Cantábrica, *Geotemas*, 13, 337-340, 2012.
- 521 Ambrose, T., Carballeira, J., López Rico, J., and Wagner, R.H.: Mapa Geológico de España E. 1:50.000, Hoja N°
522 107, *Inst.Geol. Min. España*, 1984.
- 523 Árkai, P.: Chlorite crystallinity: an empirical approach and correlation with illite crystallinity, coal rank and
524 mineral facies as exemplified by Palaeozoic and Mesozoic rocks of northeast Hungary, *J. Metamorph. Geol.*,
525 9, 723-734, 1991.
- 526 Árkai, P.: Phyllosilicates in very low-grade metamorphism: transformation to micas, in: Mottana A., Sassi, F. P.,
527 Thompson J. B., Guggenheim, S. (eds), *Micas: crystal chemistry and metamorphic petrology*, Mineralogical
528 Society of America, Blacksburg, Virginia, *Rev. Mineral. Geochem.* 46, 463-478. 2002.

- 529 Árkai, P., Horváth, Z. A., and Tóth, M.: Transitional very low-and low-grade regional metamorphism of the
530 Paleozoic formations, Uppony Mountains, NE-Hungary: mineral assemblages, illite-crystallinity, -b0 vitrinite
531 reflectance data, *Acta Geol. Acad. Sci. Hung.*, 24, 265-294, 1981.
- 532 Árkai, P., Sassi, F.P., and Sassi, R.: Simultaneous measurements of chlorite and illite crystallinity: a more
533 reliable tool for monitoring low- to very low grade metamorphism in metapelites. A case study from the
534 Southern Alps (NE Italy), *Eur. J. Mineral.*, 7, 1115-1128, 1995.
- 535 Árkai, P., Faryad, S. W., Vidal, O., and Balogh, K.: Very low-grade metamorphism of sedimentary rocks of the
536 Meliata unit, Western Carpathians, Slovakia: implications of phyllosilicate characteristics, *Int. J. Earth Sci.*,
537 92, 68-85, doi:10.1007/s00531-002-0303-x, 2003.
- 538 Árkai, P., Sassi, F.P., and Desmonds, J. 2007. 5. Very low- to low-grade metamorphic rocks. Recommendations
539 by the IUGS Subcommittee on the Systematics of Metamorphic rocks, Web version of 01/02/07, 2007.
- 540 Ayllón, F., Bakker, R.J., and Warr, L. N.: Re-equilibration of fluid inclusions in diagenetic-anchizonal rocks of
541 the Ciñera-Matallana coal basin (NW Spain), *Geofluids*, 3, 49-68, doi: 10.1046/J.I468-8123.2003.00048.X,
542 **2003.**
- 543 Bastida, F., Brime, C., García-López, S., and Sarmiento, G.N.: Tectonothermal evolution in a region with thin
544 skinned tectonics: the western nappes in the Cantabrian Zone (Variscan belt of NW Spain), *Int. J. Earth. Sci.*
545 (*Geol. Rundsch.*), 88, 38-48, doi: 10.1007/s005310050244, 1999.
- 546 Bastida, F., Brime, C., García-López, S., Aller, J., Valín, M. L., and Sanz López, J.: Tectonothermal evolution of
547 the Cantabrian Zone (NW Spain), in: *Palaeozoic conodonts from northern Spain*, editors: García-López, S.,
548 and Bastida F., *Cuadernos del Museo Geominero 1*, Inst. Geol. y Minero, Madrid, Spain, 105-23, 2002.
- 549 Bastida, F., Blanco-Ferrera, S., García-López, S., Sanz-López, J., and Valín, M.L.: Transition from diagenesis to
550 metamorphism in a calcareous tectonic unit of the Iberian Variscan belt (Central massif of the Picos de
551 Europa, NW Spain), *Geol. Mag.*, 141, 617-628, doi: 10.1017/S0016756804009653, 2004.
- 552 Battaglia, S.: Variations in the chemical composition of illite from five geothermal fields: a possible
553 geothermometer, *Clay Miner.*, 39, 501-510, doi:10.1180/0009855043940150, 2004.
- 554 Blanco-Ferrera, S., Sanz-López, J., García-López, S., Bastida, F., and Valín, M.L.: Conodont alteration and
555 tectonothermal evolution of a diagenetic unit in the Iberian Variscan belt (Ponga-Cuera unit, NW Spain),
556 *Geol. Mag.*, 148, 35-49, doi:10.1017/S0016756810000269, 2011.
- 557 Boni, M., Iannace, A., Bechstädt, T., and Gasparrini, M.: Hydrothermal dolomites in SW Sardinia (Italy) and
558 Cantabria (NW Spain): evidence for late- to post-Variscan widespread fluid-flow events, *J. Geochem.*
559 *Explor.* 69-70, 225-228, 2000.
- 560 Brime, C.: A diagenesis to metamorphism transition in the Hercynian of north-west Spain, *Mineral. Mag.*, 49,
561 481-484, 1985.
- 562 Brime, C.: Metamorfismo de bajo grado: ¿diferencias en escala o diferencias en grado metamórfico?, *Trabajos*
563 *de Geología*, 21, 61-66, 1999.
- 564 Brime, C. and Valín, M. L.: Asociaciones con cloritoide en rocas de bajo grado metamórfico de la Unidad del
565 Pisuerga-Carrión (Zona Cantábrica, NO de España), *Macla*, 6, 105-108, 2006.
- 566 Brime, C., Talent, J. A., and Mawson, R.: Low-grade metamorphism in the Palaeozoic sequence of the
567 Townsville hinterland, northeastern Australia, *Aust. J. Earth Sci.*, 50, 751-767, doi:10.1111/j.1440-
568 0952.2003.01023.x, 2003.



- 569 Brouwer, A.: Deux facies dans le Dévonien des montagnes cantabriques meridionales, *Breviora Geológica*
 570 Astúrica, VIII, 3-10, 1964.
- 571 Bucher, K. and Frey, M.: *Petrogenesis of Metamorphic Rocks*, 6th Edn. Springer-Verlag, Berlín, 318 pp, 1994.
- 572 Clauer, N. and Weh, A.: Time constraints for the tectono-thermal evolution of the Cantabrian Zone in NW Spain
 573 by illite K-Ar dating, *Tectonophysics*, 623, 39-51, <http://dx.doi.org/10.1016/j.tecto.2014.03.013>, 2014.
- 574 Colmenero, J. R. and Prado, J. G.: Coal basins in the Cantabrian Mountains, Northwestern Spain, *Int. J. Coal*
 575 *Geol.*, 23, 215-229, 1993.
- 576 Colmenero, J. R., Suárez-Ruiz, I., Fernández-Suárez, J., Barba, P., and Llorens, T.: Genesis and Rank
 577 distribution of Upper Carboniferous coal basins in the Cantabrian Mountains, Northern Spain, *Int. J. Coal*
 578 *Geol.*, 76, 187-204, doi:10.1016/j.coal.2008.08.004, 2008.
- 579 Colmenero, J.R., Vargas, I., García-Ramos, J.C., Manjón, M., Creapo, A., and Matas, J.: Mapa Geológico de
 580 España E. 1:50.000, Hoja Nº 132, Guardo, Inst.Geol. Min. España, 1982.
- 581 Corretgé, L. G. and Suárez, O.: Igneous rocks of the cantabrian/Palentine Zone, in: Dallmeyer R. D., and
 582 Martínez García, E. (eds), *Pre-Mesozoic Geology of Iberia*, *Pre-Mesozoic Geology of Iberia 72-79*, Springer,
 583 Berlin, 1990.
- 584 Corretgé, L. G., Cienfuegos, I., Cuesta, A., Galán, G., Montero, P., Rodríguez Pevida, L. S., Suárez, O., and
 585 Villa, L.: Granitoides de la Región Palentina (Cordillera Cantábrica, España), *Actas e Comunicações*, IX
 586 *Reuniao sobre a Geologia do Oeste Peninsular* (Porto, 1985), *Memorias Univ. Do Porto*, 1, 469-478, 1987.
- 587 Eberl, D. D.: Three zones for illite formation during burial diagenesis and metamorphism, *Clays Clay Miner.*, 41,
 588 26-37, 1993.
- 589 Engelder, T. and Marshak, S.: Disjunctive cleavage formed at shallow depths in sedimentary rocks, *J. Struct.l*
 590 *Geol.*, 7, 327-343, 1985.
- 591 Epstein, A. G., Epstein, J. B. and Harris, L. D.: Conodont color alteration-an index to organic metamorphism,
 592 Washington, D.C., *Geol. Surv. Prof. Pap.*, 995, 1-27, 1977.
- 593 Essene, E. J. and Peacor, D. R.: Clay mineral thermometry - a critical perspective, *Clays Clay Miner.*, 43, 540-
 594 553, 1995.
- 595 Ferreiro Mählmann, R., Petrova, T.V., Pironon, J., Stern, W.B., Ghanbaja, J., Dubessy, J., and Frey, M.:
 596 Transmission electron microscopy study of carbonaceous material in a metamorphic profile from diagenesis
 597 to amphibolite facies (Bündnerschiefer, eastern Switzerland), *Schweiz. Mineral. Petrogr. Mitt.* 82, 253-272,
 598 2002.
- 599 Fillon, C., Pedreira, D., Barbero, L., Gautheron, C., Van der Beek, P., Pulgar, J.A., and Cuesta, A.: Evidencias
 600 termocronológicas de la exhumación tectónica Oligocena-Miocena de la Cordillera Cantábrica: nuevos datos
 601 de huellas de fisión en apatitos y (U-Th)/He en circones, *GeoTemas*, 13, 1642-1645, 2012.
- 602 Frankenfeld, H.: El manto del Montó-Arauz; interpretación estructural de la Región del Pisuerga-Carrión (Zona
 603 Cantábrica España), *Trabajos de Geología*, 13, 37-47, 1983.
- 604 Frey, M.: Progressive low-grade metamorphism of a black shale formation, Central Swiss Alps, with special
 605 reference to pyrophyllite and margarite bearing assemblages, *J. Petrol.*, 19, 1, 95-135, 1978.
- 606 Frey, M.: Very low-grade metamorphism of clastic sedimentary rocks, in: Frey M. (ed), *Low temperature*
 607 *metamorphism*, Blackie, Glasgow, pp 9-58, 1987.

- 608 Frey, M., Teichmüller, M., Teichmüller, R., Müllis, J., Künzi, B., Breitschmid, A., Gruner, U., and Schwizer, B.:
609 Very low grade metamorphism in external parts of the Central Alps: illite crystallinity, coal rank and fluid
610 inclusion data. *Eclogae Geol. Helv.* 73:173-203, 1980
- 611 Gallastegui, J.: Estructura cortical de la cordillera y margen continental cantábricos: perfiles ESCI-N, *Trabajos*
612 *de Geología*, 22, 9-234, 2000.
- 613 Gallastegui, G., Heredia, N., Rodríguez Fernández, L.R., and Cuesta, A.: El “stock” de Peña Prieta en el
614 contexto del magmatismo de la Unidad del Pisuerga-Carrión (Zona Cantábrica, N de España), *Cuadernos do*
615 *Laboratorio Xeolóxico de Laxe*, 15, 203-215, 1990.
- 616 García-López, S., Brime, C., Bastida, F., and Sarmiento, G. N.: Simultaneous use of thermal indicators to
617 analyse the transition from diagenesis to metamorphism: an example from the Variscan Belt of northwest
618 Spain, *Geol. Mag.*, 134, 323–334, 1997.
- 619 García-López, S., Bastida, F., Brime, C., Aller, J., Valín, M. L., Sanz-López J., Méndez, C. A., and Menéndez-
620 Álvarez, J. R.: Los episodios metamórficos de la Zona Cantábrica y su contexto estructural, *Trabajos de*
621 *Geología*, 21, 177-187, 1999.
- 622 García-López, S., Bastida, F., Aller, J., and Sanz-López J.: Geothermal palaeogradients and metamorphic
623 zonation from the conodont colour alteration index (CAI), *Terra Nova*, 13, 2, 79-83, , 2001.
- 624 García-López, S., Blanco-Ferrera, S., and Sanz-López, J.: Aplicación de los conodontos al conocimiento de la
625 evolución tectonotérmica de las zonas externas de los orógenos, *Revista Española de Micropaleontología*, 38,
626 289-298, 2006.
- 627 García-López, S., Brime, C., Valín, M. L., Sanz-López J., Bastida, F., Aller, J., and Blanco Ferrera, S.:
628 Tectonothermal evolution of a foreland fold and thrust belt: the Cantabrian Zone (Iberian Variscan belt, NW
629 Spain), *Terra Nova*, 19, 469-475, doi: 10.1111/j.1365-3121.2007.00773.x, 2007.
- 630 García-López, S., Bastida, F., Aller, J., Sanz-López, J., Marín, J. A., and Blanco Ferrera, S.: Tectonothermal
631 evolution of a major thrust system: the Esla-VU (Cantabrian Zone, NW Spain), *Geol. Mag.*, 150, 1047-1061,
632 doi:10.1017/S0016756813000071, 2013.
- 633 Gasparrini, M., Bakker, R.J., Bechstädt, Th., and Boni, M.: Hot dolomites in a Variscan foreland belt:
634 hydrothermal flow in the Cantabrian Zone (NW Spain), *J. Geochem. Explor.* 78-79, 501-507, doi:
635 10.1016/S0375-6742(03)00115-8, 2003.
- 636 Gasparrini, M., Bechstädt, Th., and Boni, M.: Massive hydrothermal dolomites in the southwestern Cantabrian
637 Zone (Spain) and their relation to the Late Variscan evolution, *Mar. Pet. Geol.*, 23, 543-568,
638 doi:10.1016/j.marpetgeo.2006.05.003, 2006.
- 639 Gómez-Fernández, F., Mangas, J., Both, R. A., and Arribas, A.: Metallogenesis of the Zn-Pb deposits of the
640 southeastern region of the Picos de Europa (Cantabria, Spain), in: Fenoll Hach-Ali, P., Torres-Ruiz J., and
641 Gervilla F. (eds), *Current research in geology applied to ore deposits*, Univ. Granada, Granada, Spain, 113-
642 116, 1993.
- 643 Gómez-Fernández, F., Both, R. A., Mangas, J., and Arribas, A.: Metallogenesis of Zn-Pb carbonate-hosted
644 mineralization in the southeastern region of the Picos de Europa (Central Northern Spain) Province: geologic,
645 fluid inclusion, and stable isotopes studies. *Econ. Geol.*, doi:95, 19-40, 10.2113/gsecongeo.95.1.19, 2000.
- 646 Groshong, Jr R. H., Pfiffner, O. A., and Pringle, L. R.: Strain partitioning in the Helvetic thrust belt of eastern
647 Switzerland from the leading edge to the internal zone, *J. Struct. Geol.* 6, 5-18, 1984.



- 648 Guggenheim, S., Bain, D. C., Bergaya, F., Brigatti, M.F., Drits, V.A., Eberl, D.D., Formoso, M.L.L., Galán, E.,
649 Merriman, R. J., Peacor, D.R., Stanjek, H., and Watanabe, T.: Report of the Association Internationale pour
650 l'Etude des Argiles (AIPEA) Nomenclature Committee for 2001: order, disorder, and crystallinity in
651 phyllosilicates and the use of the "Crystallinity Index", *Clays Clay Miner.*, 50, 406-409, 2002.
- 652 Gutiérrez-Alonso, G., Fernández-Suárez, J., and Weil, A.: Orocline triggered lithospheric delamination, in:
653 Sussman, A.J., and Weil, A.B., (eds), *Orogenic Curvature: Integrating Paleomagnetic and Structural*
654 *Analyses: Geol. Soc. Am. Special Paper 383*, 121–130, 2004.
- 655 Gutiérrez-Alonso, G., Murphy, J.B., Fernández-Suárez, J., Weil, A., Piedad Franco, M., and Gonzalo, J.C.:
656 Lithospheric delamination in the core of Pangea: Sm-Nd insights from the Iberian mantle, *Geology*, 39, 155-
657 158, doi: 10.1130/G31468.1, 2011.
- 658 Hemley, J. J., Monteya, J.W., Marinenko, J.W., and Luce, R.W.: Equilibria in the system $Al_2O_3 - SiO_2 - H_2O$ and
659 some general implications for alteration mineralization processes, *Econ. Geol.*, 75, 210-228, 1980.
- 660 Heredia, N., Alonso, J.L., and Rodríguez Fernández, L.R. Mapa Geológico de España E. 1:50.000, Hoja N° 105,
661 Riaño, Inst. Geol. Min. España, 1997.
- 662 Heredia, N., Navarro, D., Rodríguez Fernández, L.R., Pujalte, V., and García Mondéjar, J.: Mapa Geológico de
663 España E. 1:50.000, Hoja N° 82, Tudanca, Inst. Geol. Min. España, 1986.
- 664 Heredia, N., Rodríguez Fernández, L.R., Suárez, A., and Álvarez Marrón, J.: Mapa Geológico de España E.
665 1:50.000, Hoja N° 80, Burón, Inst. Geol. Min. España, 1991.
- 666 Heward, A. P. and Reading, H. G.: Deposits Associated with a Hercynian to Late Hercynian Continental Strike-
667 Slip System, Cantabrian Mountains, Northern Spain, *Special Publications of the International Association of*
668 *Sedimentologists*, 4, 105-125, 1980.
- 669 Hosterman, J. W., Wood, G. H., and Beryin, M. J.: Mineralogy of underclays in the Pennsylvania anthracite
670 region, U.S. Geological Survey Professional Paper 700-C, C89-C97, 1970.
- 671 Hunziker, J. C., Frey, M., Clauer, N., Dallmeyer, R.D., Friedrichsen, H., Flehmig, W., Hochstrasser, K.,
672 Roggwiler, P., and Schwander, H.: The evolution of illite to muscovite: mineralogical and isotopic data from
673 Glarus Alps, Switzerland, *Contrib. Mineral. Petrol.*, 92, 157-180, 1986.
- 674 Julivert, M.: Décollement tectonics in the Hercynian Cordillera of NW Spain, *Am. J. Sci.*, 270, 1-29, 1971.
- 675 Julivert, M. : Hercynian orogeny and Carboniferous paleogeography in northwestern Spain: A model of
676 deformation-sedimentation relationships, *Z. dt. geol. Ges.*, 129, 565-592, 1978.
- 677 Julivert, M., Ramirez del Pozo, J., and Truyols, J.: Le reseau de failles et la couverture post-hercynienne dans les
678 Asturies, in: *Histoire structurale du Golfe de Gascogne*, Publications de l'Institut Français du Pétrole,
679 Editions Tech. 2, V.3.1- V.3.34, 1971.
- 680 Julivert, J. and Navarro, D.: Mapa Geológico de España E. 1:50.000, Hoja N° 55, Beleño, Inst. Geol. Min.
681 España, 1984.
- 682 Keller, M., and Krumm, S.: Variscan versus Caledonian and Precambrian metamorphic events in the Cantabrian
683 Mountains. *Z. dt. Geol. Ges.*, 144, 88-103, 1993.
- 684 Kisch, H. J.: Mineralogy and petrology of burial diagenesis (burial metamorphism) and incipient metamorphism
685 in clastic rocks, in: Larsen G, Chilingar GV (eds), *Diagenesis in sediments and sedimentary rocks*, 2.
686 Elsevier, Amsterdam, pp 289-493 and 513-541, 1983.



- 687 Kisch, H. J.: Correlation between indicators of very-low grade metamorphism, in: Frey, M. (ed), Low
 688 temperature metamorphism, Blackwell Science, Claridge, pp. 227-300, 1987.
- 689 Kisch, H. J.: Illite crystallinity: recommendations on sample preparation, X-ray diffraction settings and
 690 interlaboratory settings, *J. Metamorph. Geol.*, 9, 665-670, 1991.
- 691 Kisch, H. J., Árkai, P., and Brime, C.: On the calibration of the illite Kübler index (illite “crystallinity”),
 692 *Schweiz. Mineral. Petrogr. Mitt.* 84, 232-331, 2004.
- 693 Köberle, T., Keller, M., and Krumm, S.: Metamorphism in the southeastern corner of the Cantabrian Mountains
 694 as revealed by the Upper Devonian Murcia Quartzite, *Zbl. Geol. Paläont. Teil I*, 5-6, 447-460, 1998.
- 695 Koopmans, B. N.: The sedimentary and structural history of the Valsurvio dome, Cantabrian Mountains, Spain,
 696 *Leidse. Geol. Med.*, 26, 121-232, 1962.
- 697 Kübler, B.: La cristallinité d’illite et les zones tout à fait supérieures du metamorphism. Etages
 698 tectoniques. Université Neuchâtel à la Baconnière, Neuchâtel, Switzerland, Colloques de Neuchâtel 1966,
 699 105-122, 1967.
- 700 Kullmann, J. and Schöenberg, R.: Facies differentiation caused by wrench deformation along a deep-seated
 701 fault system (León line, Cantabrian Mountains, North Spain), *Tectonophysics*, 48, T15-T22, 1978.
- 702 Kullmann, J. and Schöenberg, R.: Facies differentiation caused by wrench deformation along a deep-seated
 703 fault system (León line, Cantabrian Mountains, North Spain)-Reply, *Tectonophysics*, 60, 308-309, 1979.
- 704 Livi, K. J. T., Veblen, D.R., Ferry, J. M., and Frey, M.: Evolution of 2:1 layered silicates in low-grade
 705 metamorphosed Liassic shales of Central Switzerland, *J. Metamorph. Geol.*, 15, 323-344, 1997.
- 706 Llorens, T., Suárez-Ruiz, I., and Colmenero J.R.: Petrografía de los carbones cantabrienses (Carbonífero sup.)
 707 del Grupo Cea de la Cuenca Guardo-Valderrueda (León-Palencia), *Geogaceta*, 40, 279-282, 2006.
- 708 Lobato, L.: Geología de los valles altos de los ríos Esla, Yuso, Carrión y Deva. Institución Fray Bernardino de
 709 Sahagún, León (C.S.I.C.), 192 pp., 1977.
- 710 Lobato, L., Rodríguez Fernández, L.R., Heredia, N., Velando, F., and Matas, J: Mapa Geológico de España E.
 711 1:50.000, Hoja N° 106, Camporredondo de Alba, *Inst. Geol. Min. España*, 1985.
- 712 López-Fernández, C., Pulgar, J. A., Gallart, J., González-Cortina, J. M., Díaz, J., and Ruiz, M.: Actividad
 713 sísmica reciente en el noroeste de la Península, 3ª Asamblea Hispano Portuguesa de Geodesia y Geofísica, 1-
 714 4, Valencia, 2002.
- 715 López-Fernández, C., Pulgar, J. A., Glez.-Cortina, J. M., Gallart, J., Díaz, J., and Ruiz, M.: Actividad sísmica en
 716 el noroeste de la Península Ibérica observada por la red sísmica local del Proyecto GASPI (1999-2002),
 717 *Trabajos de Geología*, 24, 91-106, 2004.
- 718 Maas, K.: The geology of Liébana, Cantabrian Mountains, Spain: Deposition and Deformation in a flysch area,
 719 *Leidse. Geol. Med.*, 49, 379-465, 1974.
- 720 Marcos, A.: Nota sobre el significado de la "León Line", *Breviora Geológica Astúrica*, 12, 1-15, 1968.
- 721 Marcos, A.: Facies differentiation caused by wrench deformation along a deep-seated fault system (León line,
 722 Cantabrian Mountains, North Spain)-Discussion, *Tectonophysics*, 60, 303-307, 1979.
- 723 Marcos, A. and Pulgar, J. A.: An approach to the tectonostratigraphic evolution of the Cantabrian Foreland thrust
 724 and fold belt, Hercynian Cordillera of NW Spain, *Neues Jahrb. Geol. Paläontol. Abh.*, 163, 256–260, 1982.
- 725 Marín, J.A.: Estructura del domo de Valsurbio y borde suroriental de la región del Pisuerga-Carrión (Zona
 726 Cantábrica, NO de España). Unpublished Ph. D. thesis, Oviedo University, 181 pp., 1997.

- 727 Marín, J.A., Pulgar, J.A., and Alonso, J.L.: La deformación alpina en el Domo de Valsurvio (Zona Cantábrica,
728 NO de España). *Revista de la Sociedad Geológica de España*, 8, 111-116, 1995.
- 729 Marín, J. A., Villa, E., García-López, S., and Menéndez, J. R.: Estratigrafía y metamorfismo del Carbonífero de
730 la zona de San Martín-Ventanilla (Norte de Palencia, Cordillera Cantábrica), *Revista de la Sociedad*
731 *Geológica de España*, 9, 241-251, 1996.
- 732 Marquínez, J. and Marcos, A.: La estructura de la unidad del Gildar-Montó (Cordillera Cantábrica), *Trabajos de*
733 *Geología*, 14, 53-64, 1984.
- 734 Martínez García, E., Marquínez, J., Heredia, N., Navarro, D., and Rodríguez Fernández, L.R.: Mapa Geológico
735 de España E. 1:50.000, Hoja Nº 56, Carreña-Cabrales, Inst. Geol. Min. España, 1984.
- 736 Martín-Izard, A, Palero, F.J., Regillón, R., and Vindel, E.: El skarn de Carracedo (San Salvador de Cantamuda).
737 Un ejemplo de mineralización pirometasomática en el N. de la provincia de Palencia, *Studia Geologica*
738 *Salmanticensis*, XXIII, 171-192, 1986.
- 739 Martín-Merino, G., Fernández, L.P., Colmenero, J.R., and Bahamonde, J.R.: Mass-transport deposits in a
740 Variscan wedge-top foreland basin (Pisuerga area, Cantabrian Zone, NW Spain) , *Marine Geology*, 356, 71-
741 87, <http://dx.doi.org/10.1016/j.margeo.2014.01.012>, 2014.
- 742 Merino-Tomé, O.A., Bahamonde, J.R., Colmenero, J.R., Heredia, N., Villa, E, and Farias, P.: Emplacement of
743 the Cuera and Picos de Europa imbricate system at the core of the Iberian-Armorican arc (Cantabrian zone,
744 Nord Spain: New precisions concerning the timing of arc closure. *Geol. Soc. Am. Bull.*121, 729-751, doi:
745 10.1130/B26366.1, 2009.
- 746 Merriman R. J. and Peacor D. R.: Very low-grade metapelites: mineralogy, microfabrics and measuring reaction
747 progress. In: M. Frey and D. Robinson (eds), *Low-Grade Metamorphism*, Blackwell Science, Oxford, 10-60,
748 1999.
- 749 Merriman, R. J. and Frey, M.: Patterns of very low-grade metamorphism in metapelitic rocks. In: Frey, M. and
750 Robinson, D. (eds), *Low grade metamorphism*, Blackwell Science, London, pp 61-107, 1999.
- 751 Meunier, A.: *Clays*, Springer-Verlag, Berlín, Heidelberg, New York, 2005.
- 752 Moore, D.M. and Reynolds, R. C. Jr. *X-ray diffraction and the identification and analysis of clay minerals*,
753 2nd ed., Oxford University Press, New York, 1997
- 754 Muechez, P., Heijlen, W., Banks, D., Blundell, D., Boni, M., and Grandia, F.: Extensional tectonics and the
755 timing and formation of basin-hosted deposits in Europe, *Ore Geol. Rev.* 27, 241-264,
756 doi:10.1016/j.oregeorev.2005.07.013, 2005.
- 757 Müllis, J.: The system methane-water as a geologic thermometer and barometer from the external parts of the
758 Central Alps, *B. Minéral.*, 102, 526-536, 1979.
- 759 Müllis, J., Rahn, M. K., De Capitani, C., Stern, W. B., and Frey, M.: How useful is illite “crystallinity” as a
760 geothermometer?, *Terra Nova*, 7, 128-129 (Supplement No. 1, Terra Abstracts), 1995.
- 761 Müllis, J., Rahn, M.K., Schwer, P., De Capitani, C., Stern, W. B., and Frey, M.: Correlation of fluid inclusion
762 temperatures with illite “crystallinity” data and clay minerals chemistry in sedimentary rocks from the
763 external parts of the Central Alps, *Schweiz. Mineral. Petrogr. Mitt.*, 82, 325-340, 2002.
- 764 Nijman, W. and Savage, J. F.: Persistent basement wrenching as controlling mechanism of Variscan thin-skinned
765 thrusting and sedimentation, Cantabrian Mountains, Spain, *Tectonophysics*, 169, 281-302, 1989.
- 766 Passchier, C.W. and Trouw, R. A. J.: *Microtectonics*, 2nd ed., Springer, Berlin, 366 pp, 2005.



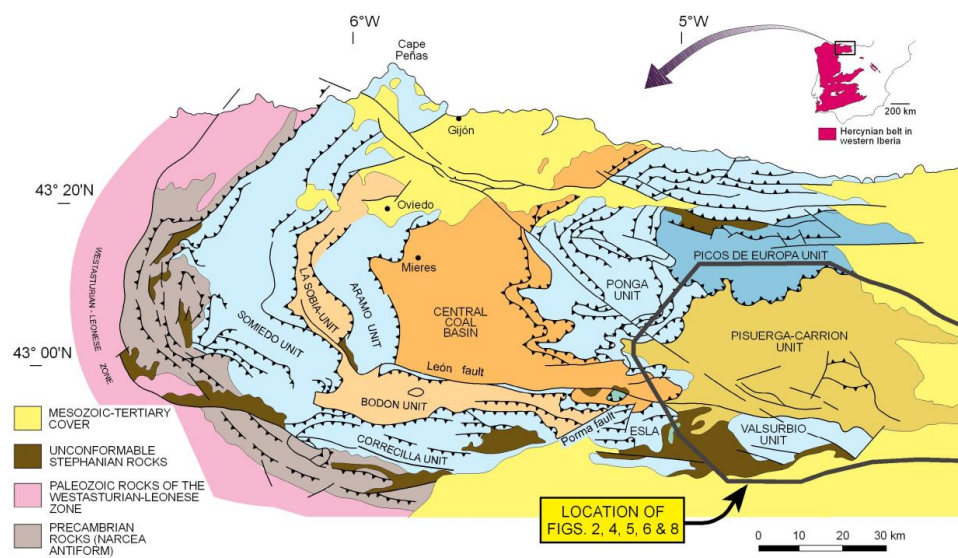
- 767 Patrick, B. E., Evans, B. W., Dumoulin, J. A., and Harris, A. G.: A comparison of carbonate mineral and
768 conodont color alteration index thermometry, Seward Peninsula, Alaska, Geological Society of America,
769 Abstracts with programs 17, 399, 1985.
- 770 Phillips, G. N.: Widespread fluid infiltration during metamorphism of the Witwatersrand goldfields: generation
771 of chloritoid and pyrophyllite, *J. metamorph. Geol.*, 6, 311-332, 1988.
- 772 Raven, J. G. M. and van der Pluijm, B. A.: Metamorphic fluids and transtension in the Cantabrian Mountains of
773 northern Spain: an application of the conodont color alteration index, *Geol. Mag.*, 123, 673-681, 1986.
- 774 Rejebian, V. A., Harris, A. G., and Huebner, J. S.: Conodont color and textural alteration: an index to regional
775 metamorphism, contact metamorphism, and hydrothermal alteration, *Geol. Soc. Am. Bull.*, 99, 471-479,
776 1987.
- 777 Rodríguez Fernández, L. R.: Evolución tectonosedimentaria del NO del Macizo Ibérico durante el Carbonífero,
778 Cuadernos do Laboratorio Xeolóxico de Laxe, 16, 37-52, 1991.
- 779 Rodríguez Fernández, L. R.: La estratigrafía del Paleozoico y la estructura de la región de Fuentes Carrionas y
780 áreas adyacentes (Cordillera herciniana, NO de España), Cuadernos do Laboratorio Xeolóxico de Laxe, Serie
781 Nova Terra, 9, A Coruña, 240 pp. 1994.
- 782 Rodríguez Fernández, L. R.: Tectónica Varisca y sedimentación sinorogénica carbonífera de la Región del
783 Pisuerga-Carrión. Guía de Campo. XIII Reunión Com. Tect. S.G.E. Inst. Geol. Min. España, Cervera de
784 Pisuerga (Spain), 85 pp, 2001.
- 785 Rodríguez Fernández, L. R. and Heredia, N.: La estratigrafía del Carbonífero y la estructura de la unidad del
786 Pisuerga-Carrión. NO de España, Cuadernos do Laboratorio Xeolóxico de Laxe, 12, 207-229, 1987.
- 787 Rodríguez Fernández, L.R. and Heredia, N.: Evolución tectonosedimentaria de una cuenca de antepaís ligada a
788 una cadena arqueada: el ejemplo de la unidad del Pisuerga-Carrión (Zona Cantábrica, NO de España), III
789 Congreso Geológico de España, Granada, Instituto Geológico y Minero de España, Simposio sobre
790 cinturones orogénicos, 65-74, 1988.
- 791 Rodríguez Fernández, L.R., Heredia, N., Navarro, D., Martínez-García, E., and Marquínez, J.: Mapa Geológico
792 de España E. 1:50.000, Hoja Nº 81, Potes. Inst. Geol. Min. España, 1994.
- 793 Savage, J. F.: Tectonic analysis of Lechada and Curavacas synclines, Yuso basin, León, NW Spain, *Leidse*.
794 *Geol. Med.*, 39, 193-247, 1967.
- 795 Sitter, L.U. de: The structure of the Southern slope of the Cantabrian Mountains, *Leidse. Geol. Med.*, 26, 255-
796 264, 1962.
- 797 Środoń, J.: X-ray powder diffraction of illitic materials, *Clays Clay Miner.*, 32, 337-349, 1984.
- 798 Suárez, O. and Corretgé, L.G.: Plutonismo y metamorfismo en las zonas Cantábrica y Asturoccidental-leonesa,
799 in: Bea, F., Carnicero, A., Gonzalo, J. C., López Plaza, M., and Rodríguez Alonso, A. D. (eds) *Geología de*
800 *los granitoides y rocas asociadas del Macizo Hespérico (libro homenaje a L.C. García de Figuerola)*, Ed.
801 Rueda, Madrid, 13-25, 1987.
- 802 Suárez, O. and García, A.: Petrología de la granodiorita de Peña Prieta (León, Santander, Palencia), *Acta Geol.*
803 *Hispanica*, 9, 154-158, 1974.
- 804 Thompson, A.P.: A note on the kaolinite-pyrophyllite equilibrium. *Am. J. Sci.*, 268, 454-458, 1970.
- 805 Theye, T., Seidel, E., and Vidal, O.: Carpholite, sudoite, and chloritoid in low-grade high-pressure metapelites
806 from Crete and The Peloponnese, Greece, *Eur. J. Mineral.*, 4, 3, 487-507, 1992.

- 807 Valverde-Vaquero, P., Cuesta, A., Gallastegui, G., Suárez, O., Corretgé, L. G., and Dunning, G. R.: U-Pb dating
808 of late Variscan magmatism in the Cantabrian Zone (Northern Spain), Meeting of the European Union of
809 Geosciences 10 (EUG 10), Strasbourg, Journal of Conference, Abstracts, 4, 101, 1999.
- 810 Van der Pluijm, B.A., and Kaars-Sijpestijn, C.H.: Chlorite-mica aggregates: morphology, orientation,
811 development and bearing on cleavage formation in very-low-grade rocks, *J. Struct. Geol.*, 6, 399-407, 1984.
- 812 Van der Pluijm, B.A., Savage, J.F., and Kaars-Sijpestijn, C.H.: Variation in fold geometry in the Yuso Basin,
813 northern Spain: implications for the deformation regime, *J. Struct. Geol.*, 8, 879-886, 1986.
- 814 Van Veen, J.: The tectonic and stratigraphic history of the Cardaño area, Cantabrian Mountains, Northwest
815 Spain, *Leidse. Geol. Med.*, 35, 45-104, 1965.
- 816 Velde, B.: Introduction to clay minerals, Chapman and Hall, 198 pp., 1992
- 817 Von Gosen, W., Buggisch, W., and Krumms, S.: Metamorphism and deformation mechanisms in the Sierras
818 Australes fold and thrust belt (Buenos Aires Province, Argentina). *Tectonophysics*, 185, 335-356
819 doi:10.1016/0040-1951(91)90453-Y, 1991.
- 820 Warr, L.N. and Rice, H.N.: Interlaboratory standardization and calibration of clay mineral crystallinity and
821 crystallite size data, *J. Metamorph. Geol.* 12, 141-152, 1994.
- 822 Winkler, H. G. F.: Petrogenesis of metamorphic rocks, 5th edition, Springer Verlag New York, 348 pp., 1979.
- 823 Zen, E-an: Metamorphism of Lower Paleozoic rocks in the vicinity of the Taconic Range in west-central
824 Vermont, *Am. Mineral.*, 45, 1-2, 129-175, 1960.
- 825



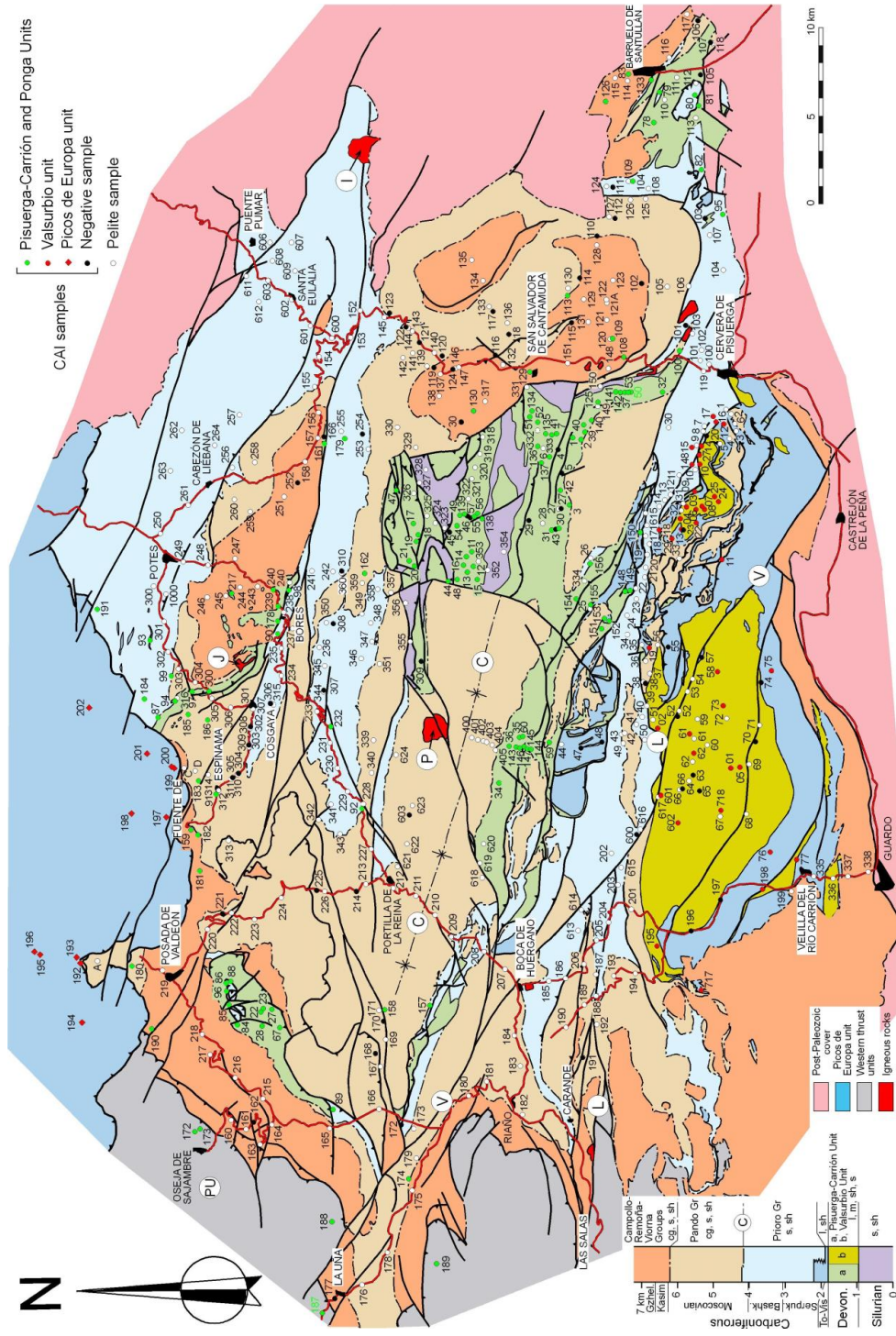
Variscan deformation	Emplacement of north-directed Palentine nappes (prior or earliest Moscovian) and the adjacent western Cantabrian nappes (late Moscovian) with associated thrusts in the PCU
Variscan deformation (cont.) (N-S shortening)	Emplacement of the south-directed Picos de Europa unit; thrusts and folds in the PCU (Kasimovian-Gzhelian) Folds and axial plane cleavage (S_1); first tectonothermal event, with deep diagenetic – low anchizone and ancaizone areas in the northern part of the PCU (late Gzhelian)
Late Variscan gravitational readjustment; extensional event	Gently dipping cleavage (S_2) associated with crosscutting folds; second tectonothermal event; very low- or low-grade metamorphism (high anchizone-epizone, and ancaizone-epicaizone) in the syncline of Curavacas-Lechada and the VU. Normal faults (latemost Gzhelian to early Cisuralian) Intrusion of igneous rocks, contact metamorphism and wide development of hydrothermal processes (Cisuralian)
Extension linked to the Basque-Cantabrian basin	Permian and Mesozoic hydrothermal episodes
Alpine deformation	N-S shortening, tightening of gentle folds, local crenulation cleavage and tilting of rocks northwards (Cenozoic).

826 **Table 1. Tectonothermal evolution of the southeastern sector of the Cantabrian Zone.**

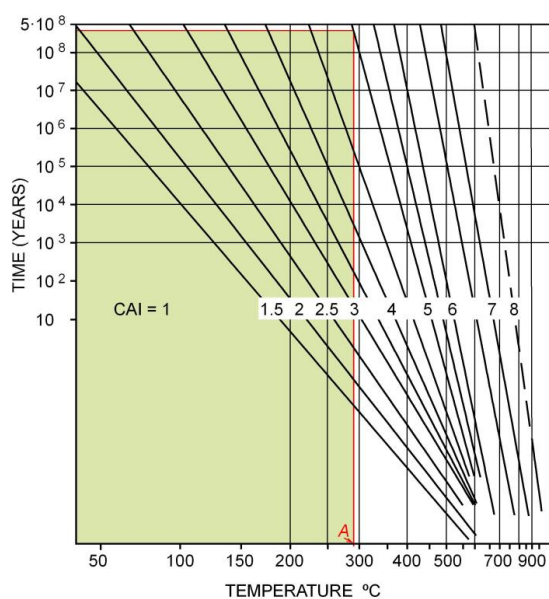


827

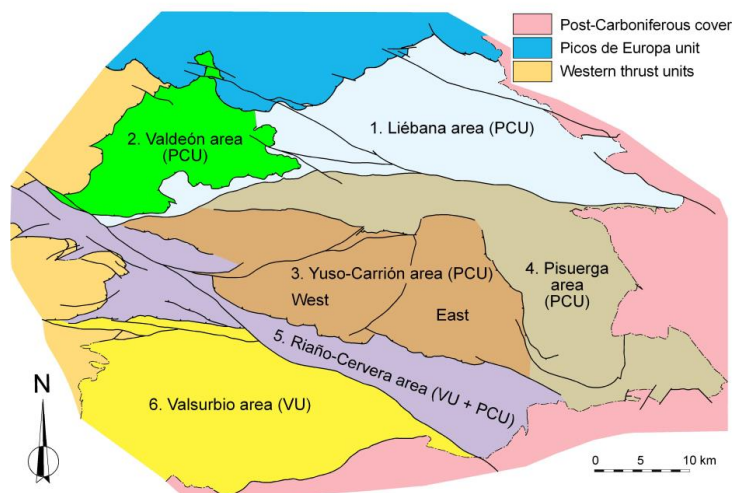
828 **Figure 1. Generalized geological map of the Cantabrian Zone (after Julivert 1971) showing major thrust**
829 **units and the location of the study area.**



831 **Figure 2. Geological map of the southeastern part of the Cantabrian Zone showing sampled localities**
 832 **(composed from Lobato, 1977; Colmenero et al., 1982; Ambrose et al., 1984; Julivert and Navarro, 1984;**
 833 **Martínez García et al., 1984; Lobato et al., 1985; Heredia et al., 1986, 1991, 1997; Rodríguez Fernández,**
 834 **1994; Rodríguez Fernández et al., 1994). Devonian and Silurian rocks of the PCU form the Palentine**
 835 **nappes. cg, conglomerate; l, limestone; m, marl; s, sandstone; sh, shale. C, Curavacas-Lechada syncline; I,**
 836 **Pico Iján granodiorite; J, Pico Jano granodiorite; L, León fault; P, Peña Prieta granodiorite; PU, Ponga**
 837 **unit; V, Ventaniella fault. Picos de Europa conodont samples after Bastida et al., 2004; Valsurbio**
 838 **conodont samples after García-López et al., 2013.**



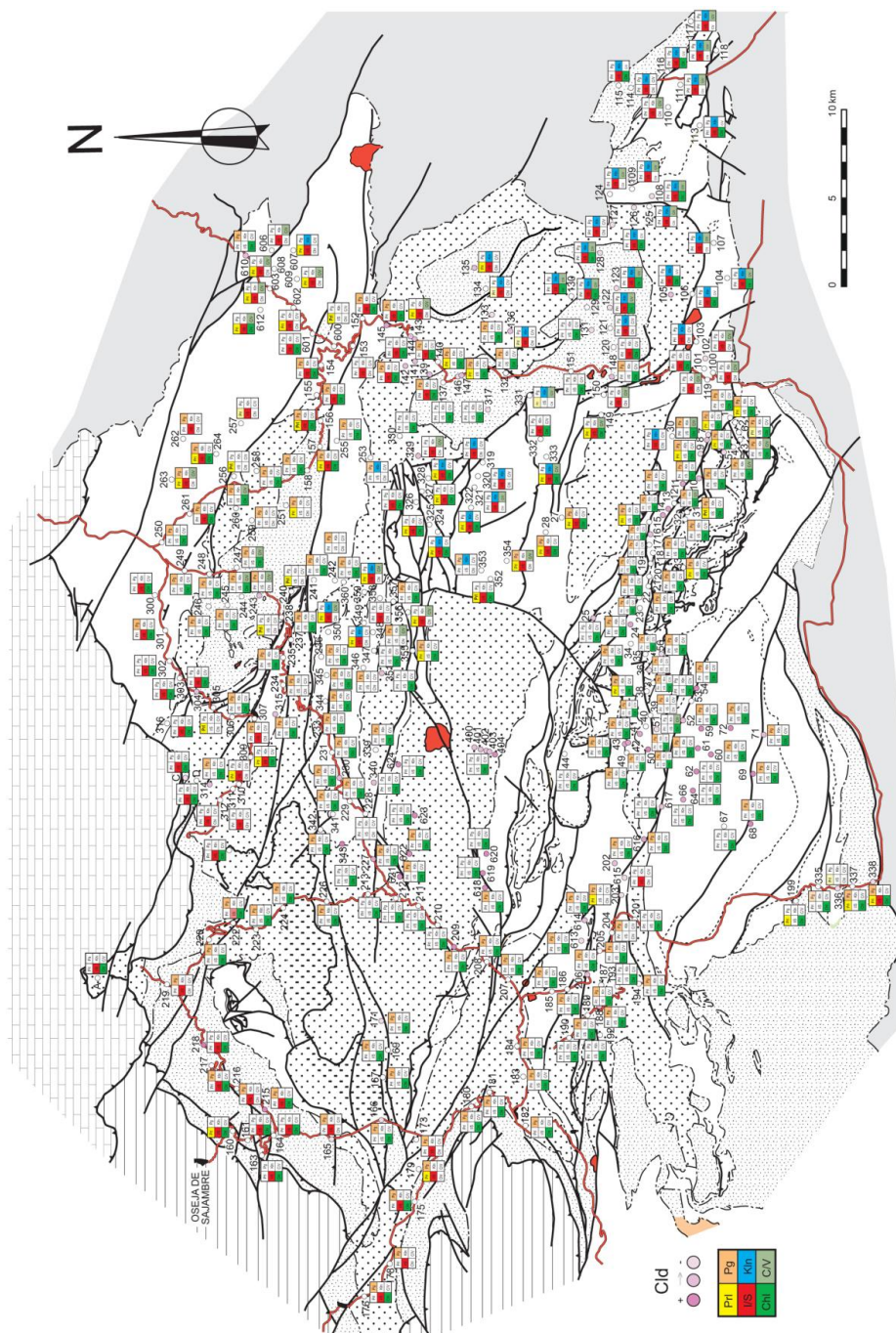
839
 840 **Figure 3. Arrhenius plot to determine paleotemperature from CAI values (on the lines) and heating time**
 841 **(from Rejebian et al., 1987). Point A indicates the minimum temperature necessary to obtain a CAI = 5 for**
 842 **a rock with an age of 400 Ma. The green area shows the temperatures and heating times unable to**
 843 **produce CAI \geq 5 in this rock.**



844

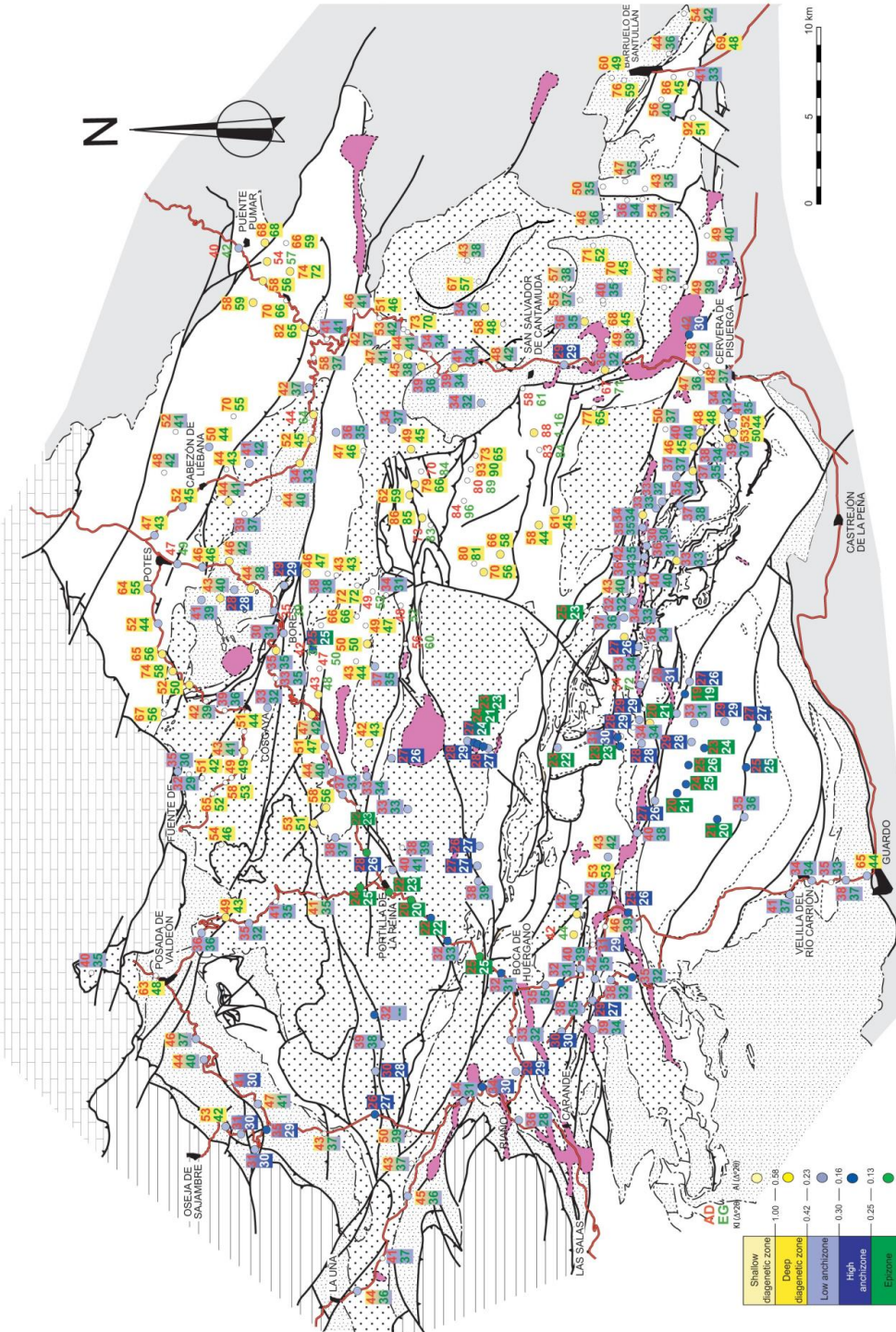
845 **Figure 4. Diagrammatic map indicating the areas in which the study units have been subdivided, following**

846 **Martín-Merino et al. (2014)**

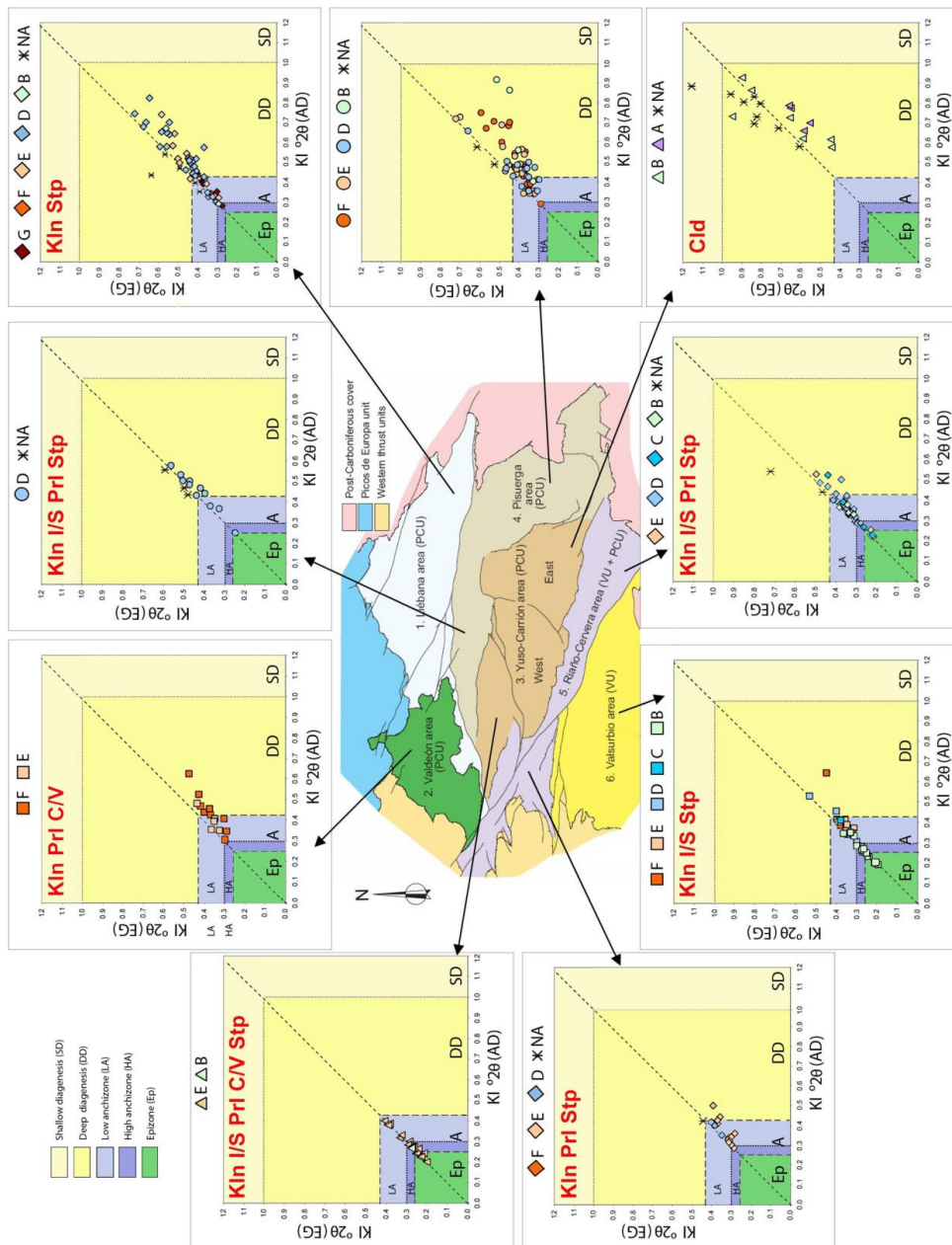


847

848 **Figure 5. Distribution of clay minerals in the study area. All the samples contain illite and therefore this**
849 **phase has not been considered in the plot. Presence of a certain phase in the sample is indicated by the**
850 **colour in the corresponding square. For legend see Figure 8.**

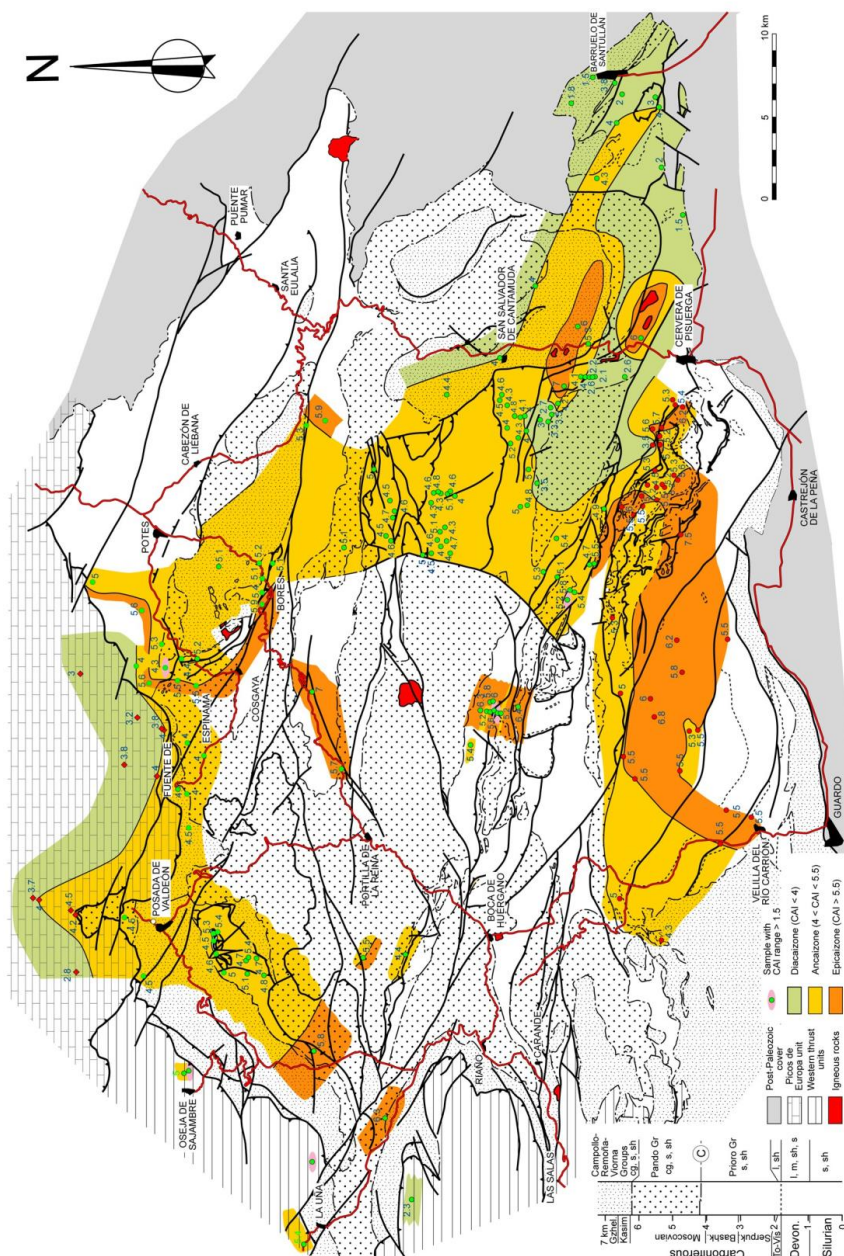


852 **Figure 6.** Map with location of Kübler Index (KI) values (Kübler scale). Upper value, in red, air dried
 853 sample; lower value, in green, sample treated with ethylene glycol. Árkai Index (AI) is indicated by the
 854 colour of the sampling point. Values corresponding to samples with significant amounts of I/S, Pr1 and/or
 855 Pg-Pg/Ms have not been highlighted with grade colours. Areas with small outcrops of intrusive rocks are
 856 shaded with purple colour. For legend see Figure 8.



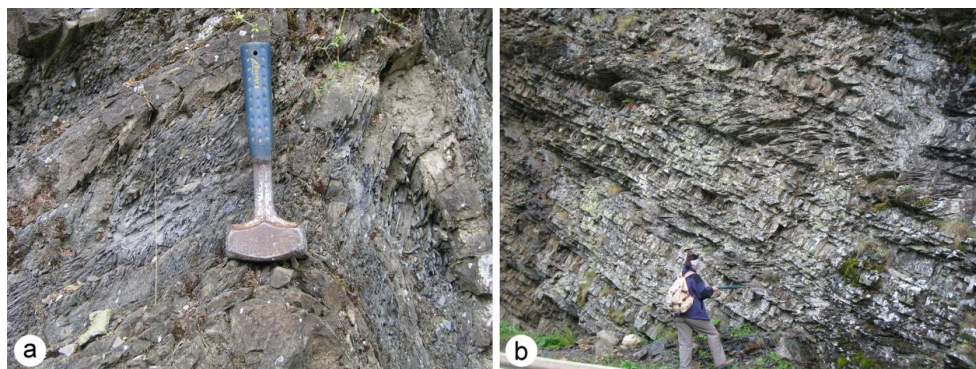


858 **Figure 7. Plot of Kübler Index (KI) measured on air dried (AD) versus KI measured on ethylene glycol**
859 **solvated samples (EG), standardized at Kübler scale. DD, Shallow Diagenesis; LA, Low Anchizone; HA,**
860 **High Anchizone; Ep, Epizone. Samples are plotted according to the areas outlined in Fig.4 and have been**
861 **grouped following the divisions of Fig. 2: A, Silurian; B, Devonian; C, Tournasian-Visean; D, Prioro**
862 **Group; E, Pando Group; F, Viorna Group; G, Campollo-Remoña Group. Samples with significant**
863 **amounts of I/S,Pr1 and/or Pg-Pg/Ms are indicated as NA (not applicable). Minerals absent in each of the**
864 **areas are indicated in red.**



865

866 **Figure 8.** Map with location of CAI values and delimitation of CAI isograds. Picos de Europa CAI data
 867 after Bastida et al., 2004; Valsurbio CAI data after García-López et al., 2013. Symbols of the CAI
 868 samples as in Fig. 2.



869
870 **Figure 9. (a) S_1 cleavage associated with a nearly upright fold (eastern part of the Liébana area; north to**
871 **the right). (b) S_2 cleavage less dipping than the bedding in a normal stratigraphic succession (Pando**
872 **Group; Curavacas-Lechada syncline; north to the left).**

873